Characterization of inflow wind fields using SpinnerLidar measurements during ScanFlow project

S.G. Koch

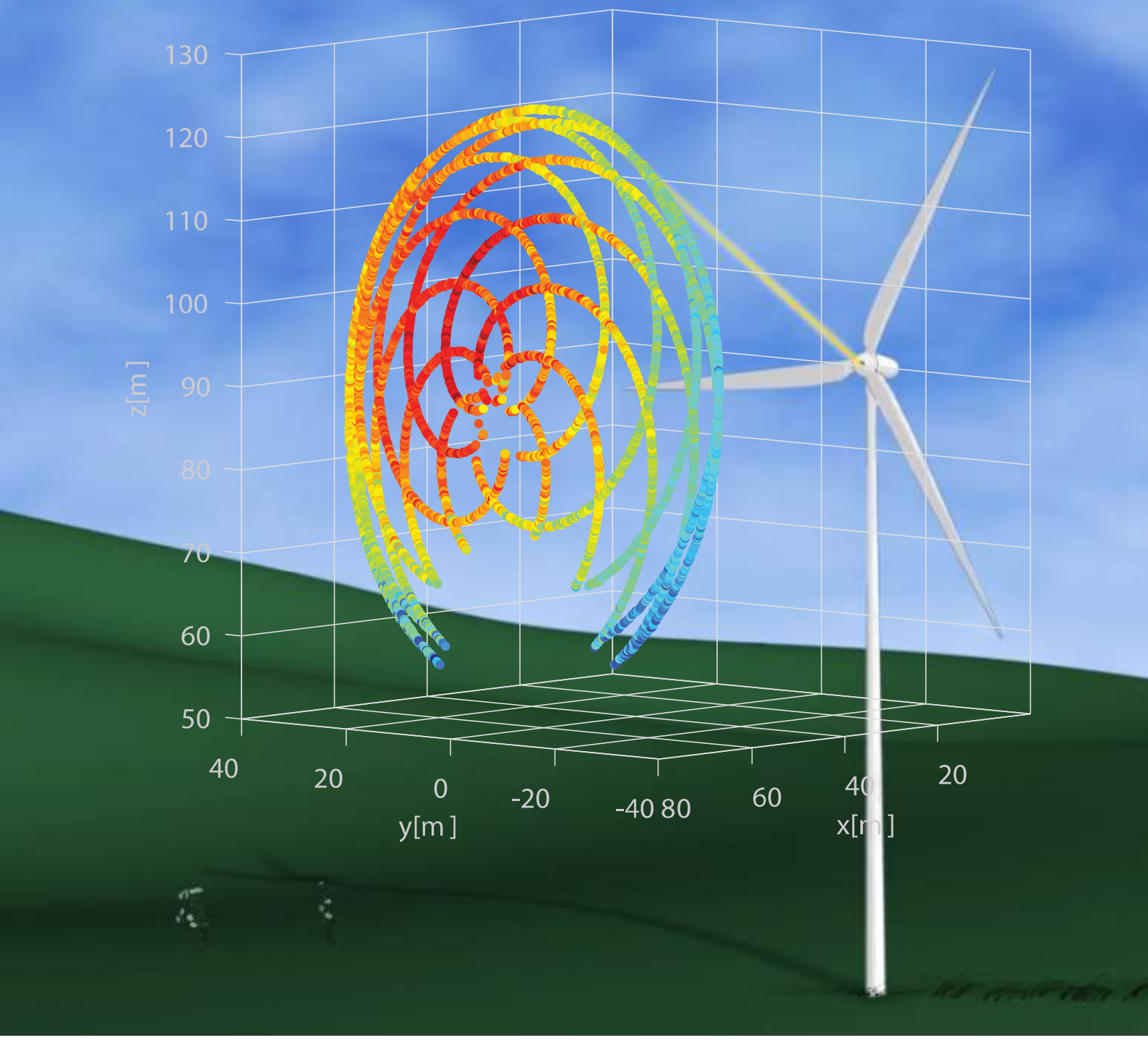

TU Delft Delft University of Technology

Challenge the future

Koninklijk Nederlands
Meteorologisch Instituut
Ministerie van Infrastructuur en Milieu

Geoscience & Remote sensing

Master Thesis

Characterization of inflow wind fields using SpinnerLidar measurements during ScanFlow project

Author:
Sam Koch
4415868

Supervisors:

Dr. S. (Sukanta) Basu	TU Delft
Prof. dr. A.P. (Pier) Siebesma	TU Delft
Dr. ir. W.A.A.M. (Wim) Bierbooms	TU Delft
Dr. J.W. (Jan Willem) Wagenaar	ECN
Dr. S. (Steven) Knoop	KNMI

September 12, 2018

Preface

This thesis has been written to fulfill the graduation requirements for the Master Geoscience and Remote Sensing at the Delft University of Technology. I have been engaged in researching and writing this thesis from September 2017 till September 2018.

The project was assigned by the Energy-research Centre of the Netherlands (ECN), where I was employed as a graduate student for 3 days a week. The Royal Dutch Meteorological Institute (KNMI) offered me accommodation and guidance for the remaining 2 days in return for collaboration and shared knowledge on this project. I can not express my gratitude enough about the interaction between these two well-known researching institutes in the Netherlands, which helped me during my thesis project.

First of all I would like to thank my two company supervisors Jan Willem Wagenaar and Steven Knoop, from ECN and the KNMI respectively, for their daily guidance and professional support during this process, not only on the researching part but also on the coaching for structuring such a thesis project. Also the help of other employees at both institutes was much appreciated. To my fellow interns I would like to say thank you for your shared support and I wish you all the best in the next steps in your careers.

Next, I would like to thank Sukanta Basu and Pier Siebesma, my supervisors from the Geoscience and Remote Sensing department at the TU Delft, for their continuous support and guidance in structuring the academic process of this thesis. Also I want to thank Wim Bierbooms, the independent member of my graduation committee, whose door was also always open for questions.

Besides my supervisors I would also like to thank Marijn Floris van Dooren from ForWind for the very useful meeting we had about our shared research, it helped me a lot.

Lastly, on a more personal note, I would like to express my gratitude to my family and friends on whom I could always count if I needed help during the whole span of my life as a student in as well Utrecht and Delft.

To all who continue reading from this point, I hope you enjoy.

Sam Koch
Delft, September 12, 2018

Abstract

The height of wind turbines continues to increase, making the need for more and higher wind measurements for wind turbine model calibrations also increase. The Energy-research Centre of the Netherlands (ECN) and the Danish Technical University (DTU) have conducted the ScanFlow campaign in the winter of 2016/2017 to study the inflow wind field of one of ECN's research turbines by deploying multiple lidar instruments. One of the instruments used in this campaign was a SpinnerLidar. A SpinnerLidar is a forward looking, nacelle-mounted, continuous wave wind lidar system. It measures Line-of-Sight components of the wind in a plane 60 meters in front of the turbine, which need to be transformed into 3D wind vectors. To do so necessary assumptions were made about the free inflow periods, namely that a vertical shear is present and that a wind direction misalignment is more likely than horizontal deviations in wind speed. With these applied assumptions the 3D wind components were determined and used in a validation study with a pulsed lidar instrument, the WindCube V2. The proposed method seems robust as a high correlation in wind speeds at hub-height between two distinctly different lidar systems was found. Using the validated SpinnerLidar measurement to find the turbulent characteristics of the free inflow wind field resulted in turbulence intensity plots showing a higher turbulent component in the lower regions of the measurement plane. Also indications for a induction zone are visible in the SpinnerLidar measurements when compared to the WindCube measurements.

Contents

List of Figures

CHAPTER 1

Introduction

1.1 Context

Wind energy is booming. Over the past few decades the amount of turbines has rapidly increased in places all over the world to harvest wind power. Searching for the highest possible capacity the turbines are increasing in size, to capture stronger winds at higher altitudes and to thereby become more cost effective. Figure 1.1 shows that from the early years of research in the 1980s to now, the turbine diameter has grown from 15 meters to over 200 meters in size (Arturo Soriano et al. [2013]).

For proper design and performance of these turbines more knowledge is needed about the wind and turbulence of the lower atmosphere. For smaller turbines meteo masts, high open-framed towers equipped with cup- or sonic-anemometers, have been sufficient. But to model the immense forces exerted on a turbine of 200 meters which generates almost 10 MW, the scarce in-situ measurements of meteo masts fall short. Luckily a new technique has made its way to the wind energy market, namely remote sensing wind lidar systems. With a very high temporal and spatial resolution, these instruments touch upon a new level of wind and turbulence data. Data which is needed to enhance the knowledge about the lower atmosphere and to improve the models which are used to design and develop the new wind turbines.

Fatigue loads on the various components of turbines are essential in determination of the lifetime of newly developed turbines. The main contributor to fatigue of the blades is not the mean wind characteristics but the turbulent component of the wind (Sathe et al. [2013]). Capturing reference measurement of these turbulent characteristics of the inflow wind field is essential in improving the wind models for design purposes.

The ScanFlow measurement campaign has been set up by the Energy-research Centre of the Netherlands (ECN) and the Danish Technical University (DTU) for better understanding of the inflow wind field of a Nordex 2.5MW research turbine and to explore some of the newly developed wind lidar systems. This research will dive into the measurements of these instruments to try to create a better understanding of the turbulent characteristics. The main focus will lie on reviewing and validating the measurements of the SpinnerLidar instrument, a continuous-wave lidar system normally installed inside the spinner of a turbine but in this campaign mounted on top of the nacelle.

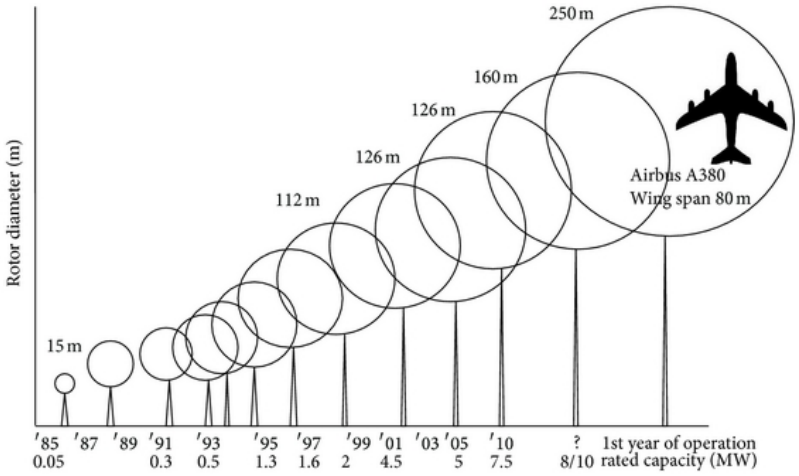

Figure 1.1: Evolution of wind turbine dimensions and power, size on the vertical axis, rated capacity in MW on horizontal axis besides 1st year of operation (Arturo Soriano et al. [2013])

1.2 Objectives

The main goal of this research is to characterize the inflow wind field with the use of measurements for the SpinnerLidar instrument. To achieve this goal three separate objectives have been determined.

The first objective to address is a quality assessment of the SpinnerLidar data. The SpinnerLidar is a new technique for measuring the inflow field of wind turbines, especially in the way it is set up in this experiment (on top of the nacelle behind the blades instead of in the rotor). A procedure has to be developed to transform the Line-of-Sight (LoS) measurements of the SpinnerLidar into 3D-wind vectors without losing information about the inflow wind field. Also the blades passing by the lidar have to be accounted for, as well as outliers in the measurements. So to sum up, the first question to be answered could be stated as:

1. *How can 3D wind vectors be constructed from SpinnerLidar data?*

Having been able to construct 3D wind vectors from the SpinnerLidar, the next question is how these measurements can be validated. Here other measurement techniques of the ScanFlow project come in. Next to the SpinnerLidar a pulsed-wave wind lidar system, WindCube, was also deployed to measure the inflow wind field. In the past decade this system has become one the two leading instruments in the field of wind lidar measurements, the other being ZephIR. A goal is to relate the measurements of the SpinnerLidar to those of the WindCube, in order to validate the SpinnerLidar as a stand-alone wind speed measurement technique.

2. *How can the SpinnerLidar measurements be (cross-)validated?*

When the measurements of the SpinnerLidar are validated and thereby a trusted measurement of the inflow wind field of the turbine can be constructed, it can be assessed in a temporal and spatial domain. For example vertical shear can be examined or the turbulent intensity of the wind. These are all quantities on which a better estimation of the inflow parameters for wind turbine design and fatigue models can be made.

3. *What are the spatio-temporal turbulent characteristics of the turbine inflow wind fields?*

CHAPTER 2

Background Theory

2.1 Remote sensing for wind energy purposes

For the performance and design of wind turbines to keep on improving, knowledge is needed about the wind profile and conditions of the site where they are located. In the previous decades the standard methodology for measuring wind profiles were meteo masts. High open-framed towers with cup anemometers installed at certain heights to make measurements of the vertical wind profile.

But recent years a new methodology has made it's entrance to the wind power market, namely remote sensing of the wind. Technologies which use either acoustic- or electromagnetic waves to 'sense' the wind at a 'remote' location. Features as wind speed, direction and physical state of the air at multiple heights can already be measured. Remote sensing applications enable measurements to be executed at greater distances, but also with a much higher spatial density.

Remote sensing of atmospheric conditions is done in two ways, either via acoustic waves or electromagnetic waves.
Acoustic waves need air as a medium to propagate. It is therefore that this technique, also known as sodar, is mostly used to detect changes in this medium, like temperature and humidity.
Remote sensing with electromagnetic waves does not need a medium and can therefore travel much further than dissipating sound waves. Lidar and radar are the two most common known applications of electromagnetic wave remote sensing. Their difference lies in the part of the spectrum in which they operate. Radar uses the microwave spectrum with a relatively large wavelength in comparison to lidar, which uses the light spectrum with a much smaller wavelength. The wavelength used is determinative for which atmospheric properties can be studied, because the size of the wavelength determines the size of the particles and structures in the air it can interact with. Lidar interacts with aerosols, where radar mostly detects water droplets. It is therefore that lidar is better usable to study wind and radar to study rain.
Figure 2.1 shows the different wavelengths for remote sensing applications of the atmosphere (Emeis [2007]).

In short, remote sensing instruments emit a power signal which then reflects on small particles in the air, called backscattering. The backscattered signal of these particles is then received by the same or a different device. Power, frequency and time can all be used to say something about the state of air particles.

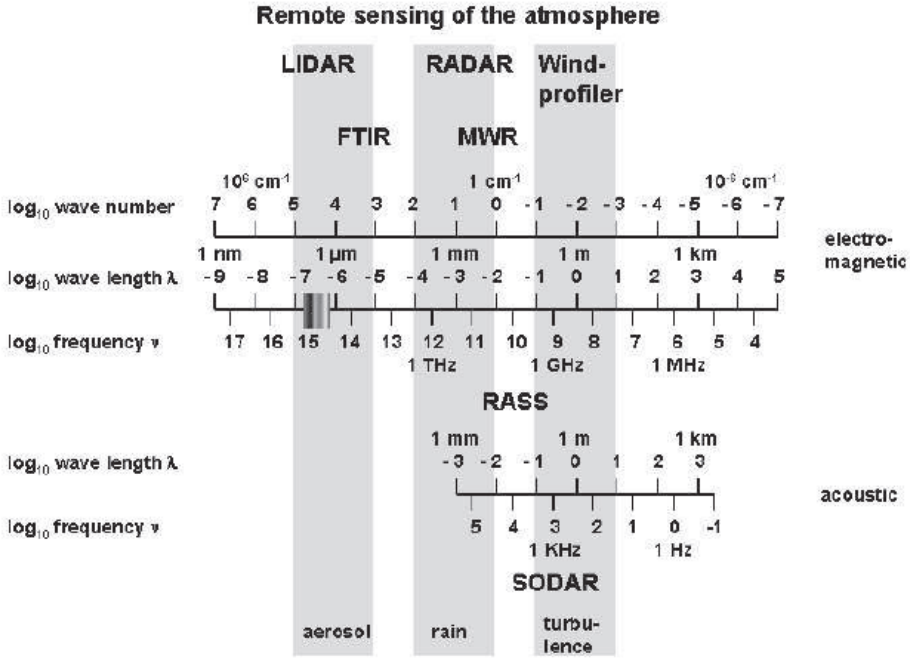

Figure 2.1: Electromagnetic (top) and acoustic (below) ground-based remote sensing techniques for probing and monitoring the atmospheric boundary layer. (Emeis [2007])

2.2 Introduction to wind lidar

LiDAR, short for Light Detection And Ranging, is a technique which uses the light spectrum of electromagnetic waves for remote sensing application. It relies on the transmission of electromagnetic energy to bounce back from an object of which the return can be analyzed to determine information about the object that was hit. Like the name says it is commonly used for detection and ranging. For example, the travel time of light from the instrument to the object and back can be used to determine the distance to the object.

For wind speed measurements, lidar is a bit more complicated to use, because air does not automatically reflect the light signal. Fortunately the air usually contains aerosols and other particles such as dust, water droplets, pollutants and salt crystals which are well suited for wind speed remote sensing, as they are small and suspended in the air and therefore drifting along at the speed of the wind. To detect such small particles, the used electromagnetic waves need to have a small wavelength to cause scattering. Typical wind lidars use wavelengths of around 1.55 μm, which causes the received light to be Mie scattered back towards the lidar instrument. Radar uses a larger wavelength and can therefore not detect these small particles. However, measuring wind speed with radar is possible in the case of rain, but still smaller turbulent structures will be overlooked with this technique.

Experiments with wind lidar started already in the 1970s, but it was not until after the telecommunication-boom of the 90s, which introduced fiber optics, that the first commercial all-fiber wind lidar, the ZephIR, became available in 2003/2004 in Ledbury, UK (Mikkelsen et al. [2013]). For determination of the wind speed by lidar a special technique is needed. Travel time and power of the reflected signal can only tell something about the distance and state of the reflected object. But for determination of the speed the so-called Doppler effect is needed, this will be further explained in section 2.4

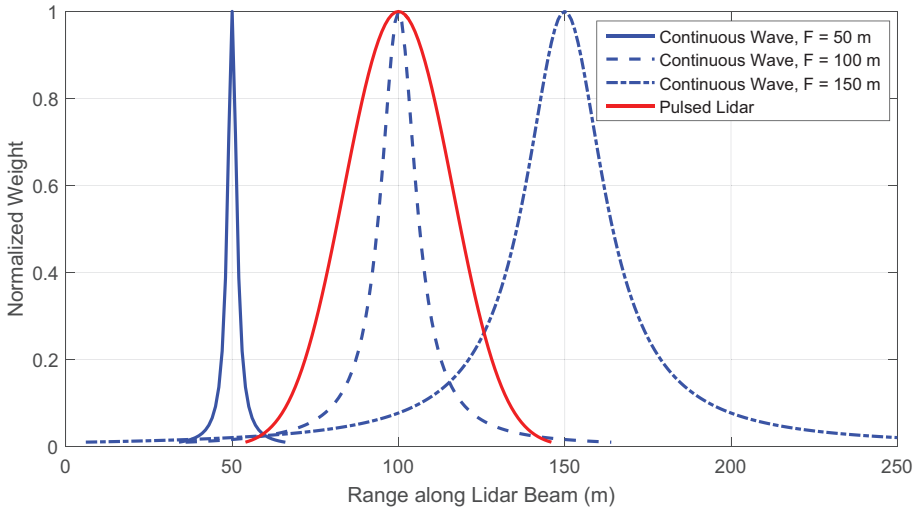

Figure 2.2: Normalized range weighting functions for a continuous-wave (CW) lidar with focus distances of 50 m, 100 m, and 150 m as well as a pulsed lidar. (Simley et al. [2018])

2.3 Different lidar types

In the field of wind lidar techniques two broad categories can be distinguished: coherent lidar and direct detection lidar. Both techniques rely on the Doppler shift of the returning signal but the way this shift is measured differs. Coherent lidar makes use of a reference beam, which is used to compare against the returning Doppler-shifted signal. Combined these signals cause a so-called light beating, where the slightly shifted frequencies resonate to create a beating which is representative to the Doppler shift. Direct detection lidar makes use of an optical filter, such as a Fabry-Perot etalon, to determine the frequency of the returned signal. It often operates in the ultra-violet spectrum and can therefore exploit the scattering at molecular level, making this technique less reliable on the presence of aerosols in the air.

Most commercially available wind lidar techniques make use of the coherent lidar technique. Within coherent lidar another subdivision can be made between continuous and pulsed lidar systems. Both systems differ principally in terms of temporal and spatial resolution, influencing the abilities to measure and resolve mean wind speeds and turbulence characteristics of the wind.

As the name says, continuous-wave (CW) lidar emits an uninterrupted laser beam which is focused at a predetermined measurement distance. There it determines, continuously, the Doppler shift in the detected backscatter from that specific distance. To get measurements from multiple distances the lidar instruments needs to be refocused every time it changes to a different measurement location. The range and spatial resolution are determined by the focal properties of the system's telescope. Shorter distances have a higher accuracy for range and spatial resolution due to the fact that in these cases the focal distance is smaller, and thereby also the sampling volume. As the focus distance increases the range weighting function also changes, in a way that more spatial averaging occurs further away from the instrument. The range weighting function is proportional to the square of the focus distance. Continuous-wave lidars are therefore often limited to distances shorter than 200 meters.

Pulsed lidar systems emit an interrupted laser beam, typically with an effective pulse length of 30 meters. It detects the backscattered light from particles at different distances as the pulsed laser propagates further with the speed of light. Multiple measurements are obtained at specific range-gated distances from one single emitted beam. The spatial resolution is independent of measurement range as this system does not need to focus a lens on a preset distance. The range is determined by the power and width of the emitted pulse, as this determines the amount of deterioration of the laser as it travels further and also the power of the backscattered signal. The Carrier-to-Noise ratio (ratio between backscattered pulsed signal and noise) is dependent for the maximum measurement distance it can achieve, making pulsed

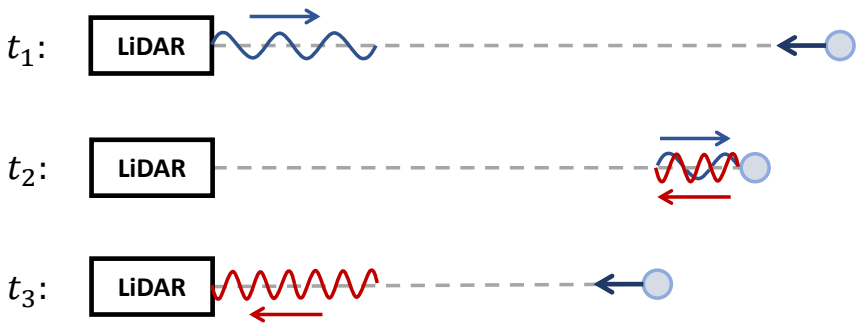

Figure 2.3: Schematic display of Doppler effect as used in wind lidar systems. At t_1 a light beam with a standard frequency is emitted toward a moving air particle, instants later at t_2 the light beam interacts with the moving air particle causing a backscattering reflection with a higher frequency, at t_3 this reflection is measured by the same lidar instrument.

lidar systems very dependent on the state of the atmosphere. Newly developed pulsed lidar systems can reach distances of a few kilometers in perfect conditions (Floors et al. [2016]).

Figure 2.2 shows the different range weighting function for CW and pulsed lidar systems (Simley et al. [2018]). As can be seen the spatial averaging for CW lidar systems is better in the shorter range, under 200 meters, than the pulsed lidar systems. But beyond this point pulsed lidar systems will be able to keep a constant spatial resolution if atmospheric conditions allow measurements to be taken far away.

For this research measurements will not be taken beyond a distance of around 70 meters for a continuous-wave lidar system (SpinnerLidar) and 140 meters for a pulsed-wave lidar system (WindCube V2).

2.4 Doppler shift to wind speed

The Doppler-effect is a well-known occurrence in physics. The perfect example is that of a passing ambulance, of which the tone will lower at the moment it passes. In the same way, an object that is moving while it is emitting or reflecting some sort of sound or light wave, compresses the wave that is emitted forward and stretches one that is emitted backwards. For lidar purposes this means that when air particles are moving towards the instrument the backscattered light will have a higher frequency (blue shift) and vice versa if air particles are moving away from the instrument the frequency of the backscattered light will lower (red shift). See Figure 2.3 for a schematic display of the Doppler effect as used in wind lidar. In case the air particles are moving exactly perpendicular to the laser emitted by the lidar, the backscattered light will have no frequency shift because it is not moving from or toward the instrument. This reveals one of the main problems of single beam lidar wind measurements, namely that it can only measure one LoS component of true 3D wind speed. This phenomenon is known as the Cyclops syndrome and will be discussed later on (Schlipf et al. [2011]).

A coherent lidar uses the beat phenomenon to determine the Doppler shift of the backscattered light. The beat phenomenon occurs when two waves with almost, but not exactly, the same frequencies are combined. As can been seen in Figure 2.4 two waves with frequencies that are slightly off have a constructive and destructive effect on each other in the resulting wave. The combined wave tends to 'beat' in power in the exact same frequency as the difference between the two initial frequencies.

Inside a coherent lidar instrument a part of the transmitted beam is split to function as a reference beam for the received, Doppler shifted, backscattered light. These two beams combined cause a beating which can be monitored to find the Doppler shift between the two beams. The Doppler shift, Δf_d, proportional to the line-of-sight movement of the air particle towards or away from the lidar, is defined by,

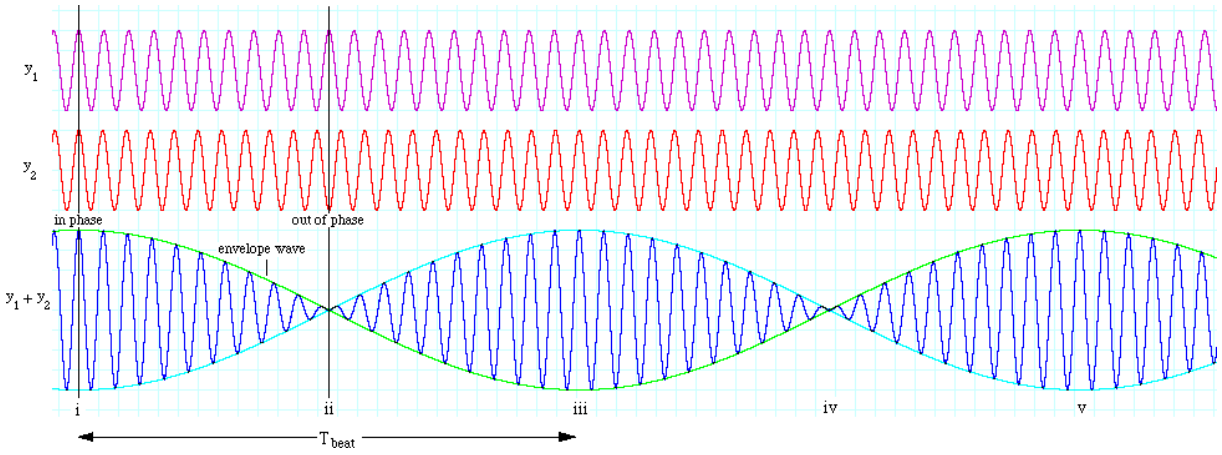

Figure 2.4: Beat phenomenon showing the envelope wave (green) of the combined wave ($y_1 + y_2$) to have a beating period T_{beat}

$$\Delta f_D = \frac{2V_{LOS} f_L}{c} \tag{2.1}$$

where V_{LOS} is the component of the particle's velocity in the direction of the laser beam, c is the speed of light and f_L is the frequency of the emitted laser. The factor 2 considers that Doppler shifts are caused by waves at the location of moving particles and secondly by the particles scattering radiation back to the lidar (Hofmeister et al. [2015]). A simple example of this equations shows that, with a near-infrared laser with a wavelength of 1.5 µm, which equals a frequency of 200 THz, and a line-of-sight velocity of 1 m/s, the change in frequency due to the Doppler shift becomes only 1.3 MHz (note the three order change).

It has to be mentioned that the beat frequency method can not distinguish between positive or negative Doppler shifts, meaning it can not see if air particles are moving away or towards the instrument. In a case where a wind lidar is facing up from the ground this can make a crucial difference in the determination of the wind direction, but in the case of this study, where a wind lidar is mounted on top of a nacelle and has a horizontal field of view into the direction of the wind, it can be assumed that wind is always moving towards the turbine.

2.5 Ground-based versus nacelle-mounted

The most common application of wind lidar system is still from a ground-based perspective. With the lidar looking up, a large range of vertical measurements can be conducted in the same way a meteo mast would be measuring a vertical wind profile. Ground-based is practical in a way that the lidar instrument is easy to move around doesn't require any structures to measure up to heights of 200 meters. However, a downside of being ground-based is that the looking direction of the lidar instrument is vertical and the main wind flow is horizontal. Single beam lidar systems can always only measure the wind speed component of a moving particle in the exact same direction as the laser beam, more about this in section 5.1.3. That is why ground-based lidar systems always scan in a conical way, to increase the angle between the looking direction main wind direction. But this introduces a new problem, namely volume averaging. Every horizontal disk the lidar system scans needs to be averaged as if conditions are equal over the whole disks, which they are not. This becomes a problem when smaller scale turbulent structures are of interest, these are lost due to the averaging. Especially higher up, where the averaging volume is very large. Still ground-based wind lidar is getting very reliable for average wind speeds and longer time period statistics, it is just not that favorable of turbulence research.

An upcoming trend in the last years is mounting a lidar instrument on its side on top of a nacelle. In this way the looking direction of the lidar is in almost the same direction as the wind flow (because a

turbine is always yawing into the wind). This means that the component of the true wind speed which will be measured is very large and almost equal to the true wind speed. Therefore, when applied with the correct algorithms, almost all individual measurements can be considered as wind speed measuruments. This makes it potential for turbulence research much better.
The SpinnerLidar is such an instrument which is looking straight into the wind direction. Still for this methodology transformations have to be applied, but this will also be further discussed in section 5.1.3

2.6 Prospects of wind lidar

Meteo masts with installed cup- or sonic-anemometers have been the standard for decades for a reason. When installed in a place of interest they provide a very constant and accurate measure of the wind profile at the location of the tower. The temporal resolution is very high and also the determination of the measurement locations is very precise. Furthermore cup- and sonic-anemometers have been tested vigorously in wind tunnels to correct for instrumental errors. Before the emerging of remote sensing technologies these so-called in-situ measurements where the only way of measuring wind. But now that remote sensing becomes more and more available and the need for knowledge about the wind becomes higher, a few disadvantages of in-situ measurements come to light.

First of all in a spatial sense. The permanent location of a meteo mast is good for the precision of the location of a measurement, but makes it very limited in measuring with a higher spatial coverage. Of course in the vertical way this is dependent on the amount of anemometers installed, but in the horizontal way it will always stay insufficient. In comparison, wind lidars can be relocated quite easily and can also measure at multiple locations from one set-up. With a range up to 200 meters for continuous-wave lidars and even a few kilometers for pulsed-wave lidars (Floors et al. [2016]), the spatial coverage is much higher. If a wind lidar system is nacelle mounted (like the SpinnerLidar) it has the extra advantage that the measurement location can automatically follow the wind direction as the turbine is turning into the wind. This is particularly useful in studies about the inflow or wakes of wind turbines.

Another disadvantage of meteo masts is considered in the costs of installation. With the turbines getting bigger, meteo masts will also have to reach higher to obtain measurements in the upper part of the wind profile, but building masts up to 200 meters can be very expensive. Only a few meteo masts ranging over 200 meters, like Cabauw in the Netherlands, are constructed in Europe, most are only around 100 meters high. Installing meteo masts offshore is even more costly. Wind lidars can be easily deployed at nearly any location and can also be redeployed in multiple campaigns.

2.7 Turbulence assessment with wind lidars

The possibilities for wind lidar to replace the in-situ meteo masts seem forthcoming, but there are still some doubts within the wind energy research community about the performance of wind lidars. As of 2017 the IEC standard 61400-12-1 report includes a paragraph about wind lidar measurements for wind turbine site research. It is still very basic, lidars may only be used in flat terrain with a reference meteo mast of about 30 meters close by. This fact adds to the belief that wind lidars are becoming more accepted within the wind energy research community, but then only for average wind speed and direction measurements. For short time and spatial scaled turbulence wind lidars will still need more testing as for to become fully reliable.

Measuring mean wind speeds over a longer time scale, as most ground-based lidars do, enables the instruments to filter out the faulty measurements and construct a reliable average value. Measuring turbulence however, requires solid individual measurements to capture all small scale structures of the turbulent wind. One way to give a measure to turbulence of the wind is using the turbulence intensity.

$$I = \frac{\sigma_u}{\bar{u}} \tag{2.2}$$

This quantity uses multiple individual measurements over a certain period of time to construct a standard deviation for the wind during this period, σ_u. This standard deviation itself of course tells something about the variance of the wind, hence the turbulence. But if divided by the average wind speed of the same period, $\bar{u}$, the quantity is scaled for the effect of increasing absolute variance with increasing wind speeds.

Turbulence intensity seems a good variable to use if one wants to asses turbulence from lidar data. However, it is very dependent on where the measurements of the lidar are taken. In the case of ground-based lidars, volume averaging plays a significant role in determining wind speeds at greater heights. If measurements from multiple locations are needed to be averaged over a volume to get a correct wind speed measurement, turbulent structures smaller than this volume can never be detected. Here nacelle-mounted lidars might give a way out. As nacelle-mounted lidars need less volume averaging to determine correct wind speeds, these individual measurements can be used to determine turbulence intensity at small spatial scales, and might thereby still be able to capture small turbulence structures.

An attempt to capture these smaller turbulent structures with the use of nacelle-mounted lidar is done in this research. With the little research being conducted on this topic it will be difficult to compare the findings with other studies. But with this attempt the knowledge about measuring turbulence with lidar systems will increase, making it worthwhile to present the findings.

CHAPTER 3

Literature Review

3.1 Validation studies on wind lidar instruments

3.1.1 Ground-based lidars estimating turbulence statistics

The International Energy Agency Wind Implementing Agreement (IEA) has quite recently released a report about the possibilities to estimate wind turbulence with lidar applications. In this study they summarize several campaigns about wind lidars in the previous decade to see if they can meet the standards of turbulence research (Sathe et al. [2015])

In 2009, a campaign was held in Høvsøre, Denmark, to study the variance in post-processed lidar data from a ground-based continuous-wave lidar (ZephIR) and pulsed-wave lidar (WindCube). For both these instruments the data was processed using the Velocity-Azimuth-Display (VAD) strategy, which basically implies that conical scans are being performed by the instruments to be able to average over a horizontal distance in order to determine a three component wind vector. In this study the post-processed measurements were also compared against the measurements of a sonic-anemometer installed at a height of 100 meters in a nearby met mast. Figure 3.1 shows the comparison of mean wind speeds for both instrument. It can clearly be seen that the systematic error, indicated by the linear fit, and the uncertainty in the measurements, indicated by the value of R^2, are both very small, because both values are within 2% of the value 1. This would prove that both instruments can measure accurate mean wind speeds at a height of 100 meters. Being able of measuring correct mean wind speeds and measuring actual small scale turbulent structures is not the same. But with this validation being successful Sathe et al. [2015] make the suggestion that there is no reason not to continue with trying to look at turbulence analysis from these wind lidar instruments.

In the end of the report it is concluded that turbulence analysis is possible with lidar measurement, but not on every length scale. Due to the larger averaging volumes of ground-based lidar instruments, the smaller scale characteristics could not be captured in the measurements. Even though the sampling rate of lidars is increasing rapidly, the spatial averaging will always overshadow the smaller scale turbulent structures.
However, smart processing schemes and new techniques are being developed which might enable even the smaller structures in turbulence to be captured.
For larger scale turbulent structures the contemporary lidar instrument have shown very confident results in multiple ground-based lidar studies executed over the past few years.

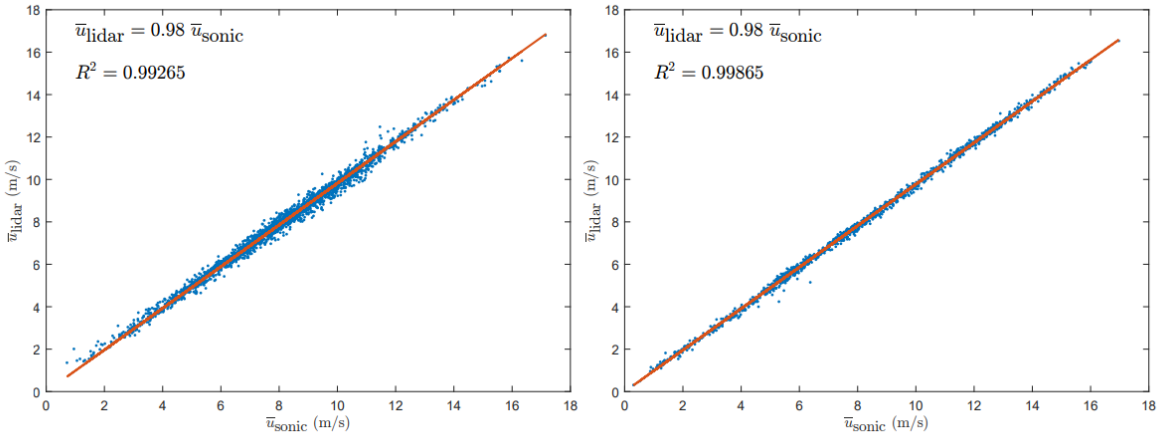

(a) CW lidar (b) Pulsed lidar

Figure 3.1: Regression analysis of lidar mean wind speed measurements and sonic anemometer mean winds peed measurements, (a) Continuous-wave lidar system with a R^2 value of 0.992, (b) Pulsed-wave lidar system with a R^2 value of 0.998 (Sathe et al. [2015])

3.1.2 LAWINE project executed by ECN

In June 2014 ECN executed a campaign for turbulence assessment with two ground based lidars, both WindCube V2's, at the ECN Wind turbine Test site Wieringermeer (EWTW). Since turbulence intensity measurement with ground based lidars requires special attention, the study focused on making a turbulence assessment against a meteo mast equipped with sonic- and cup-anemometers (Bot [2014]).

As a result it was concluded that the results from the lidars were in better agreement with the sonic-anemometers than with the cup-anemometers. Especially in the lower regions of the wind profile the cup-anemometer measured lower turbulence intensity than the lidars and sonic-anemometers. But this was explained as being a result of the response time of the cups, caused by their inertia, which reduces the variance at vastly changing wind speeds near the surface.

Comparing the sonic-anemometers and the lidars resulted in slightly higher turbulence intensity values for the lidars, but not much. The trend of the curves over height were very similar which would therefore indicate a small calibration error. Also the results of the two lidar instrument were in very good agreement, demonstrating the high reproducibility of lidar systems.

Figure 3.2 shows one of the resulting turbulence intensity plots of the LAWINE campaign. The turbulence intensity is here plotted as a function against the mean wind speed for each of the three measurement devices. It can be seen that with lower average wind speeds the turbulence intensity is increasing, however, from about an average of 3 m/s the turbulence intensity stays practically constant around a value of 0.1. As said before, the three instrument shows very similar trends and only tend to differ a bit in magnitude.

3.1.3 Wind field reconstruction from nacelle-mounted lidar

Besides the fact that nacelle-mounted lidars do not average over large volumes and are therefore better suited for turbulence measurements, the problem of LoS measurements remains. For every single beam lidar set up it will always remain necessary to use a method which condenses the raw lidar measurements into useful wind field characteristics such as speed, direction and vertical gradient (wind shear).

Borraccino et al. [2017] developed a method to estimate wind field characteristics by using model-fitting wind field reconstruction techniques on raw nacelle lidar measurements, where a wind model was combined with a simple induction model. The method was applied to two experimental datasets from a five-beam Demonstrator and ZephIR Dual Mode lidar system. It allowed for robust determination of free inflow

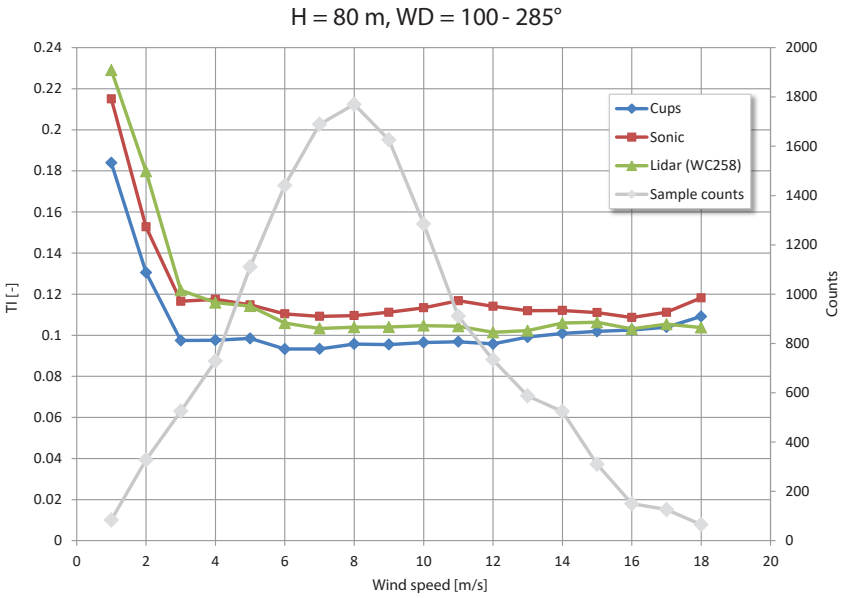

Figure 3.2: Comparison of turbulence intensities measured with cup and sonic anemometers and a ground based LiDAR (WC258) at 80 m height during the LAWINE campaign (Bot [2014])

wind characteristics as the reconstructed wind speeds were within 0.5% of the wind speed measured by a reference meteo mast. It used 10 minute averaged data to fit the LoS measurements to first only an assumed wind model and later a combined wind and induction model. It was only after implying the induction model that the best results were obtained.

3.2 Previous SpinnerLidar research

The SpinnerLidar is a continuous-wave lidar instrument normally installed inside the turbine's spinner, hence the name. The instrument was developed by DTU and first deployed in 2009 (Angelou et al. [2010]), and has since still been under further development. A more detailed description of the instrument and it's installation in this particular research will be given in section 4.3. But here a quick overview will be given about previous research the SpinnerLidar has been involved in.

3.2.1 UniTTe WP3 campaign

Angelou and Sjöholm [2015] conducted a campaign with the objective to make a detailed mapping of the upwind flow in front of a turbine. But instead the main goal of this study shifted towards addressing the processing of SpinnerLidar data.

Prior to installing the SpinnerLidar in this campaign it was necessary to estimate the accuracy of the measurement locations acquired by the SpinnerLidar in a controllable environment. By focusing the SpinnerLidar on a wall and measuring the difference of the measurement locations to a reference beam the instrument could be adjusted for it's internal offsets.

Also in this research for the first time the SpinnerLidar was installed behind the turbine's blades on top of the nacelle, instead of in the spinner. A few approaches were developed to filter the measurements for blade reflections.
In this campaign the exact location and direction with respect to the turbine blades was determined during installation of the SpinnerLidar, this knowledge in combination with the rotation speed of the turbine could be used to predict when the blades could cause blind spots in the measurement data. Another

approach relies on the maximum speed return the blades can give when passing by the instrument which could be used as a low-pass filter.

At the end of the UniTTe WP3 campaign a comparison was made between the measurements of the SpinnerLidar and a sonic anemometer installed in a nearby meteo mast. For this estimation the radial wind speeds at the center of the measurement plane was considered as always being horizontal and in the exact wind direction. The comparison showed a very significant relation between the two instruments which encouraged further research with the SpinnerLidar.

3.2.2 Cyclops syndrome

As mentioned before a single beam lidar instrument as the SpinnnerLidar can only measure a LoS component of the true 3D wind vector. This is often referred to as the 'Cyclops syndrome'. Section 5.1.3 and 5.1.4 will explain further the true origin of this problem and will also describe the method used in this research to tackle the Cyclops syndrome.
But with the application of the SpinnerLidar in several studies over the past few years other approaches have already been designed to solve this problem.

One of these methods relies on a fast computational fluid dynamics model designed to fit to the raw measurement data. The CFD model used is a coded Fourier version of the linearized Navier-Stokes equations with conservation equations for mass and momentum, called the 'LINCOM CFD solver'. All LoS measurements are used as input to define this CFD model, which in its turn can then be regarded as a model of the true 3D wind field (Mikkelsen et al. [2016]).
This approach has shown promising results, but a down-side is that it is very dependent on the boundary conditions used in the CFD model.

Another method suggests to make use of practical wind parameters to describe the general wind conditions. A five parameter wind model is proposed to characterize the mean behavior of a three dimensional wind vector field. These parameters being, averaged wind speed, linear horizontal shear, linear vertical shear, averaged horizontal stream direction and averaged vertical stream direction. Only three LoS measurements are needed to solve this system of nine nonlinear equations for these five parameters (Kapp and Kühn [2014]).
The benefit of this methods is that with more measurements the accuracy of the five parameters increases. But a downside can be that information about individual measurements is lost by this approach.

CHAPTER 4

Measurement Set-up

4.1 ScanFlow project

The ScanFlow project has been executed under the framework of the Integrated Research Program for Wind Energy (IRPWind) commissioned by the European Union. IRPWind is a consortium of 24 partners, who are all European research institutions and universities working in the field of wind energy research. With this program the European Commission has made it possible to accelerate the collaboration and ambitions in this project.

In the summer of 2014 IRPWind did its first call for Joint Experiments, to which ECN and DTU responded with the ScanFlow Project.
The Technical University of Denmark (DTU) is contributing strongly to the Danish wind energy research environment, which is internationally recognized as being in the forefront of wind energy technology. DTU Wind Energy is a world-class research institute within theoretical and applied wind energy. It operates in several state-of-the-art remote sensing wind observation technologies, like for example the WindScanner.eu project.
The Energy research Centre of the Netherlands (ECN) is an independent research organization which has as goal to develop and achieve a better energy market technology for a more sustainable future. The ECN Wind Energy department has developed an impressive track record over the last 40 year in research, high quality measurements and consultancy in the wind energy sector. Furthermore ECN facilitates a wind turbine test field, which has executed numerous standardized measurement campaigns in the framework of wind turbine certification and development.

Together, DTU and ECN executed the ScanFlow Project during the winter of 2016/2017. The aim of the project was to measure the incoming wind field in front of a wind turbine using scanning LiDARs and create a state-of-the-art inflow dataset that can be used for evaluation of aerodynamic models. For this multiple LiDAR systems have been used, including a single SpinnerLidar, three short-range WindScanners and a WindCube V2, which also allows the possibility of cross-referencing these instruments. The main deliverable of the ScanFlow Project was to make the obtained data publicly available for scientific research, which has been done through an open access e-science platform also available beyond project time on irpwind-scanflow.eu.

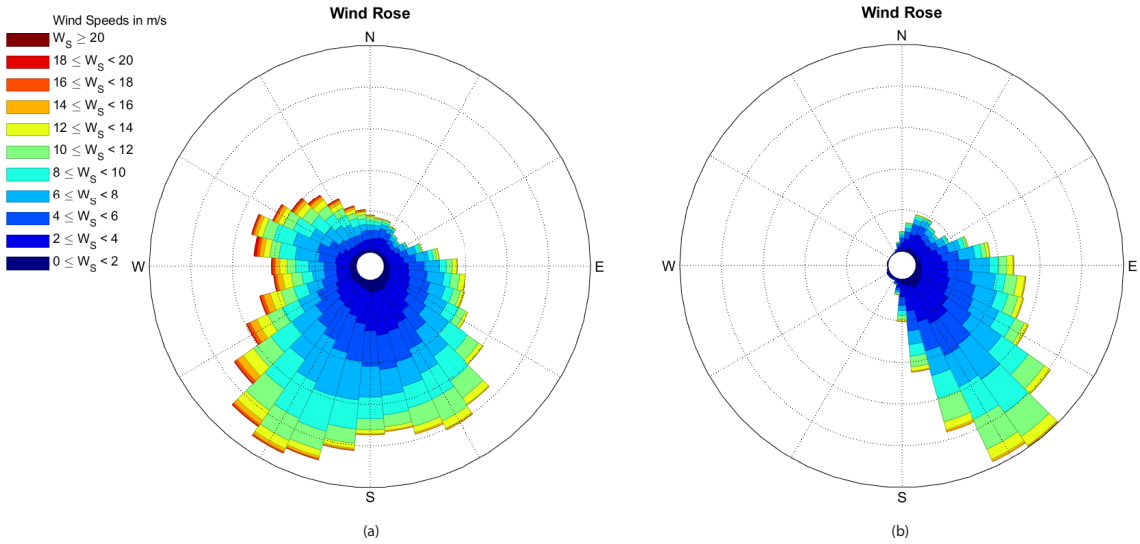

Figure 4.1: Windrose of measurements of R9 wind vane during ScanFlow campaign, (a) total windrose of all measurement data during campaign, (b) selected moments when wind was arriving at turbine from free inflow conditions (see Section 4.5)

4.2 ECN test site facility

As mentioned briefly before, ECN facilitates a wind turbine test site, called the ECN Wind turbine Test site Wieringmeer (EWTW), which allows full scale wind turbine and wind farm related research. The test site consists of flat, agricultural terrain with occasionally rows of trees and a few farm houses. It is located at approximately 500 meters from the IJsselmeer near the town of Wieringerwerf, where the average wind speed at a height of 80 meters is 7.5 m/s from a main wind direction of the South-West (Wagenaar [2017]).

On the site are five modern, full-scale research turbines (Nordex) with a hub height and rotor diameter of 80m and rated power of 2.5 MW. The turbines are located in a row from West to East, on a line from 95 to 275 degrees, and labelled R5 to R9. From these five turbines, R9 was subject to the measurement campaign of the ScanFlow project. This turbine was chosen because there are other prototype turbines located to the South of this row of turbines, which influence the inflow during Southerly wind. Also at the time of the campaign, other experiments were being conducted on R5, R6 and R7. R9 was the only turbine, which in case of Easterly winds has a completely free inflow. Especially in winter periods, when the wind is more likely to come from the East than in summer periods, R9 had the highest change of receiving this free inflow.

The windrose on the left of Figure 4.1 shows the wind direction and speeds as measured by the wind vane on top of turbine R9 during the whole span of the ScanFlow measuring campaign. As can bee seen the dominant wind direction during this period is from the South. Normally more wind would also come from the West and less from the East, but as this campaign was conducted during winter more South-Easterly winds were present.

4.3 SpinnerLidar

The SpinnerLidar is a continuous-wave remote sensing instrument, developed in a cooperation between DTU and ZephIR (a wind LiDAR manufacturer). The name 'spinner' would suggest the instrument to be installed inside the spinner of the turbine, which has in previous campaigns been the case, however in the ScanFlow project due to practicalities the SpinnerLidar has been placed on top of the nacelle behind

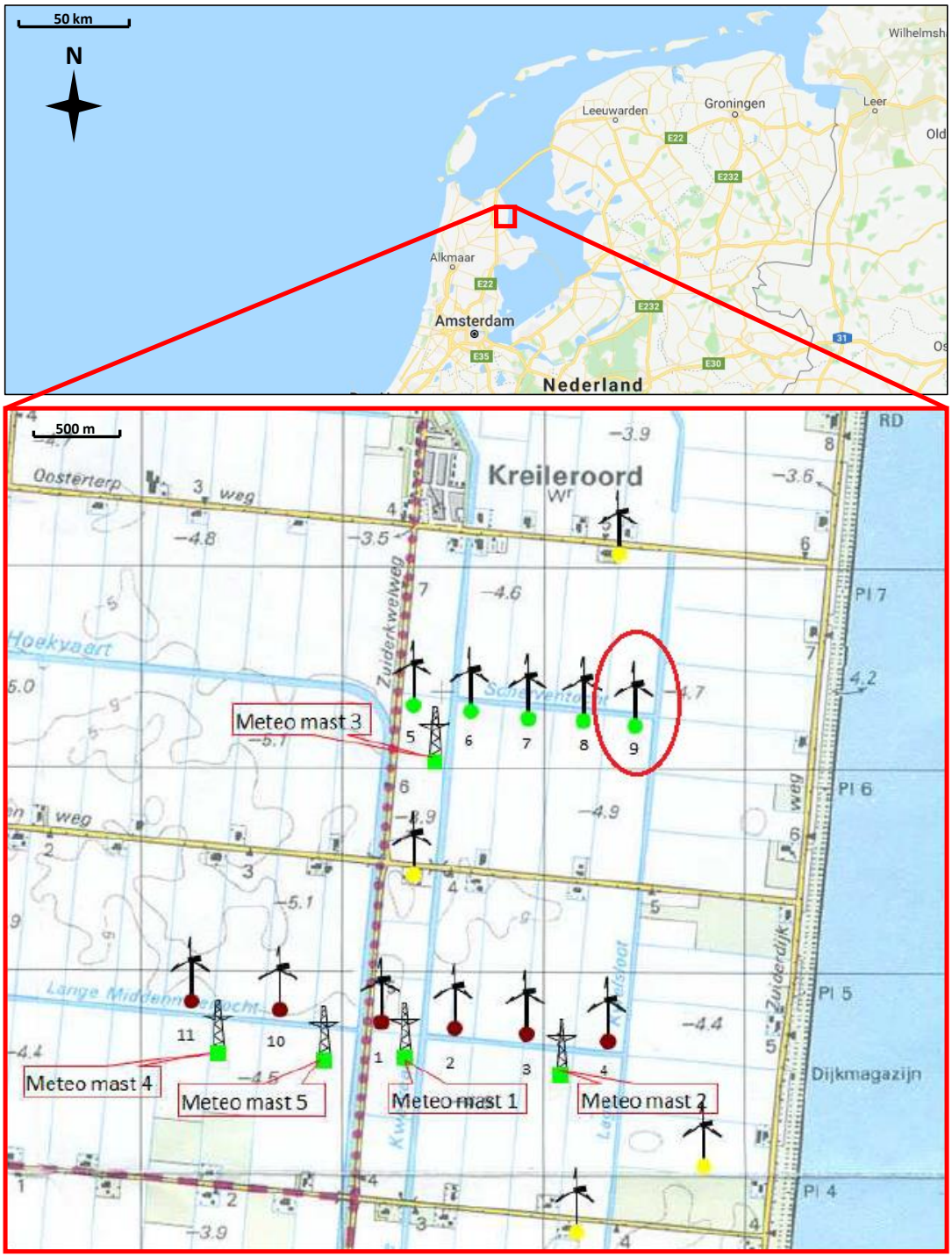

Figure 4.2: Map of ECN Wind turbine Test site Wieringermeer (EWTW), turbine 9 (red circle) is the turbine used in this research, which is part of a row of five research turbines (5-9). To the South are six prototype turbines, also the different meteo masts are indicated.

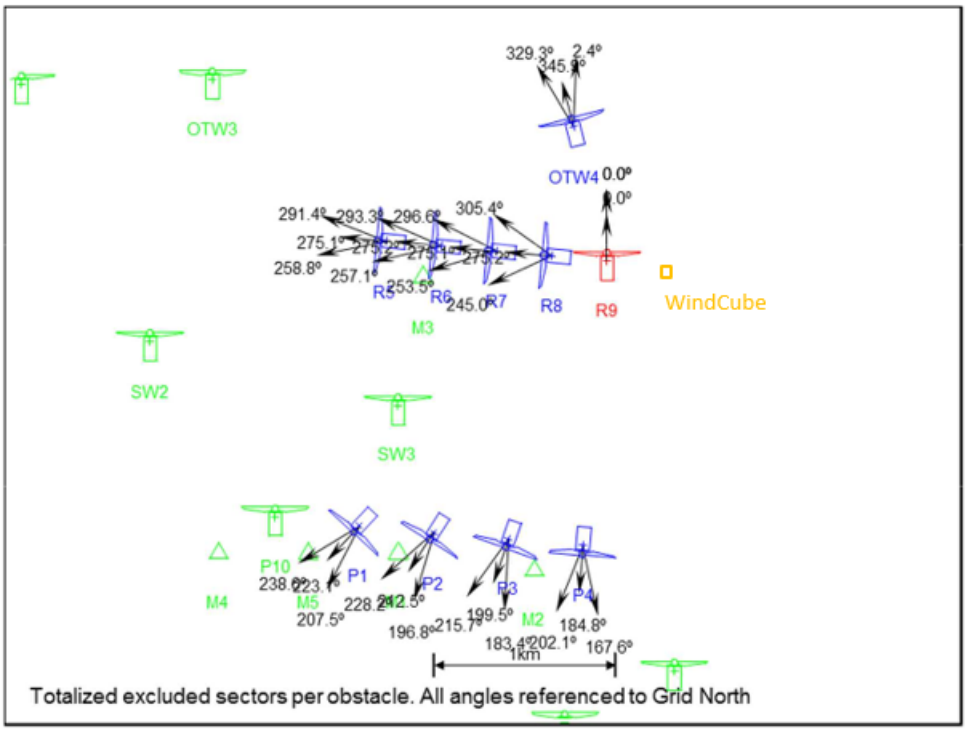

Figure 4.3: Site plan of EWTW showing wake angles for turbine R9 (red), as calculated following IEC standard 61400-12-1. As can be seen turbine R9 will receive free inflow between 2.4 and 167.6 degrees. R5 to R9 are ECN Nordex test turbines, P1 to P4 are other prototype turbines, M indicates the different locations of meteo masts. (Werkhoven et al. [2017])

the wind turbine's rotor. The SpinnerLidar is based on a normal upward looking Zephir LiDAR, but has been placed on its side in order to scan horizontally.

Another difference between a normal upward looking wind LiDAR and the SpinnerLidar is that the scanner-head of this one has two optical prisms instead of one, rotating both at a constant speed, with a fixed ratio between their speeds of 13/7. This combination of prisms makes the SpinnerLidar scan with the typical rose curve structure as can be seen in Figure 5.1. This structure was chosen as the best applicable method to scan homogeneously with installing just two simple prisms.
While it is following this path, it measures with a sampling frequency of exactly 400.2305328 Hz. As a result of this configuration the location of each measurement is not the same for every reoccurring second, but shifts every time the SpinnerLidar starts a new cycle.

The SpinnerLidar was mounted in a dedicated frame on top of the nacelle, so that together with the height of the turbine the scanning head was located about 82.9 meters above the surface. As mentioned in the previous chapter a continuous wind LiDAR instrument has to be focused at a specific distance in order to retrieve continuous backscatter from this distance. Here the SpinnerLidar was focused at a distance of around 71 meters. Combining this with the fact that the instrument was placed 8.0 meters behind the turbine's rotor, the spherical plane which was continuously scanned was at approximately 63 meters in front of the rotor. A note has to be made here, as it was discovered that in the earlier stage of the campaign the SpinnerLidar was not constantly focused, due to settings of a previous campaign the focus distance changed between 70 and 100 meters. Luckily this was discovered in time to adjust the SpinnerLidar for the rest of the campaign and the data of the first few weeks could be manually corrected. Inside the SpinnerLidar the returned back-scatters from the aerosols are converted to wind speed measurement by use of the earlier described beat phenomenon.

Eventually all the data from the SpinnerLidar was put in a database format containing the following variables (See Appendix A for an example):

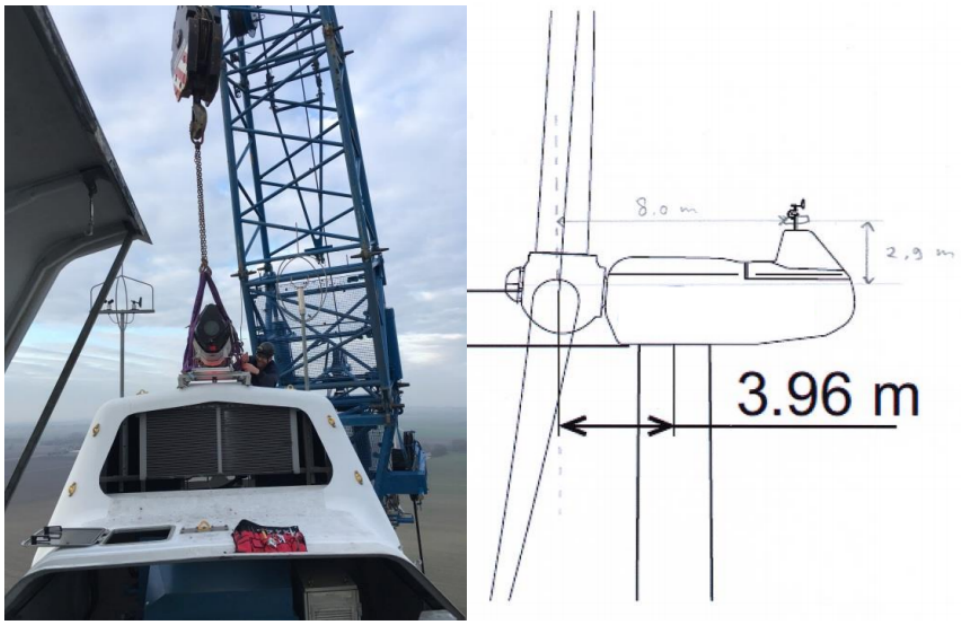

Figure 4.4: Installation of SpinnerLidar instrument on top of Turbine R9, the scanner-head was located 8.0 meters behind the rotor blades and 2.9 meters above hub height

- **Azimuth,** Θ_{Spin} [1] **[degrees]**
  Azimuth angle of the orientation of the instrument itself measured wit an internal leveller. (So not the azimuth angle of the measurement locations)
- **Focus [meters]**
  The distance from the scanning head of the SpinnerLidar to the point where the measurement laser beam is focused.
- **Inclination,** Φ_{Spin} [1] **[degrees]**
  Inclination angle of the orientation of the instrument itself measured wit an internal leveller. (So not the inclination angle of the measurement locations)
- **Power**
  The total signal power in the whole thresholded Doppler spectrum.
- **Quality**
  A quality measure ($0 \leq Q \leq 1$) of the speed estimate. It is defined as the ratio between the signal power around the estimated frequency of the thresholded Doppler spectrum, to the total power in the whole thresholded Doppler spectrum.
- **Sx**
  The projection of the unit vector along the line-of-sight measurement direction on the SpinnerLidar internal x-axis.
- **Sy**
  The projection of the unit vector along the line-of-sight measurement direction on the SpinnerLidar internal y-axis.
- **Vlos [m/s]**
  The wind speed component along the line-of-sight measurement direction.

The data was stored on a 10 minute base. Creating .csv files containing over 290,000 measurement points for each 10 minute period during the whole campaign.

[1] When referred to further on in this report these variables will be indicated by these symbols

Figure 4.5: Location of WindCube V2 instrument 200 meters to the East of Turbine R9

4.4 WindCube

The WindCube V2 is a more well-known and tested instrument in the field of wind research. It is a small cubical instrument which can be placed in any location to measure a wind profile. Where the SpinnerLidar makes use of a continuous-wave lidar, the WindCube uses pulsed lidar to simultaneously measure wind speeds at binned heights. The WindCube was set to measure at every 10 meter interval between 40 and 130 meters from the surface. For every height it collects continuous data which is binned on a basis of 10 minutes, after which it returns an averaged value for every 10 minute period at every height level.

The data of the WindCube was saved in a .csv file which contained the following interesting variables for every height level at every 10 minute period (See Appendix B for an example):

- **Data_Avail [%]**
  Data Availability of measurements. A quality measure based on the Carrier-To-Noise-Ratio of the return.
- **Wd [degrees]**
  Average horizontal wind direction
- **Ws [m/s]**
  Average horizontal wind speed
- **WsDisp [m/s]**
  Horizontal wind speed standard deviation
- **ZWs [m/s]**
  Average vertical wind speed
- **ZWsDisp [m/s]**
  Vertical wind speed standard deviation

The WindCube was located 200 meters to the East of the turbine R9, at a direction angle of 81 degrees. The same reason holds here as for choosing the most Easterly located turbine, chances on free inflow are highest here.

4.5 Data Availability

The data availability of the SpinnerLidar reaches from 17 to 26 December and from 16 January to 7 February. Due to a power loss from the end of December till the half of January no measurements were stored in this period. As mentioned before during the month December the SpinnerLidar seemed to be configured different than in the last month of the campaign. The focus distance is changing from 70 tot 100 meters every second in the first 3 weeks of data from the campaign. For comparison (Chapter 6) of the two instruments this was not considered as a problem, because measured wind speed and direction will stay the same. However, for characterization (Chapter 7) these first weeks of measurements were disregarded as a changing focus distance and therefore measurement location will have an effect on the variance of the wind speeds.

The WindCube has been operational the whole 2.5 months of this ScanFlow campaign. However, the WindCube is of course also dependent on retrievals of backscattered light to measure wind speeds. During occasions when there are too few aerosols in the air, or when rain or mist is blocking the light beams, the WindCube will automatically flag it's measurements as less valid.

Eventually the availability of both instruments has to be combined to be able to compare the measurements. As will be showed in the next chapter these will be the moments of free inflow for both instruments.

CHAPTER 5

Wind field reconstruction

5.1 SpinnerLidar Data

5.1.1 Coordinate System

As mentioned the Spinnerlidar has a sampling frequency of around 400 Hz, meaning the instruments sends a light beam to 400 unique points in space every second. The location of these points is stored in an internal, left-handed coordinate system which is described by only two variables, Sx and Sy. These two coordinates can be considered as a projection of the unit vector in the line-of-sight direction of the beam on the internal x- and y-axis of the instrument. Sz is not stored but can, if needed, be calculated from these two variables ($\sqrt{Sx^2 + Sy^2 + Sz^2} = 1$). DTU has also written a document which explains the internal coordinate system of the SpinnerLidar, this document can be found in Appendix C. Sx and Sy can be used to express the coordinates in a spherical coordinate system instead of a Cartesian coordinate system, by

$$\Theta = sin^{-1}(Sx), \quad \Phi = sin^{-1}(Sy) \tag{5.1}$$

where Θ is a measure for the azimuth direction, and Φ a measure for the inclination, both seen from the middle of the viewing direction.
In the data file also two variables Θ_{Spin} and Φ_{Spin} are found, which are a measure for the angle of the viewing direction of the instrument. In order to come up with the corrected azimuth and inclination for every point these variables have to be added to the previously determined internal angles.

$$\Theta_{corr} = \Theta + \Theta_{Spin}, \quad \Phi_{corr} = \Phi + \Phi_{Spin} \tag{5.2}$$

After applying this correction it is very important to notice that the whole internal coordinate system of the SpinnerLidar is rotated 90 degrees. It can be said that the whole instrument was laying on its side, and that it is still a left-handed coordinate system. In order to rotate the internal coordinate system to coordinates which represent the real worlds (right-handed) coordinate system. The following conversion had to be applied:

$$\Theta_{real} = -(-\Phi_{corr})^1, \quad \Phi_{real} = \Theta_{corr} \tag{5.3}$$

Beyond this point in this research when azimuth or inclination is mentioned it can always be considered as a reference to Θ_{real} and Φ_{real} respectively.

[1] One minus sign is for rotating the coordinate system, the other for making it a right-handed system instead of left-handed

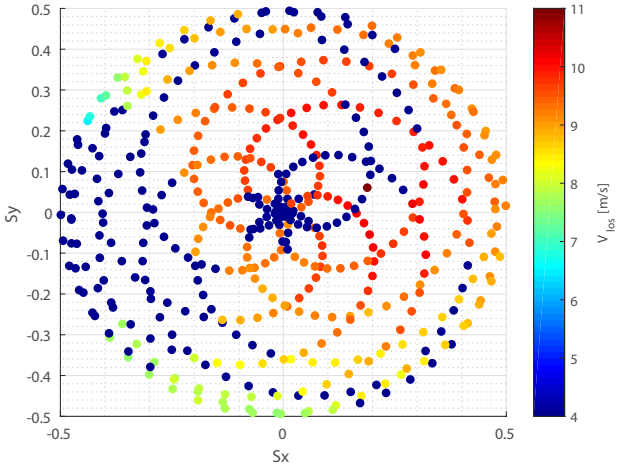

Figure 5.1: One second of data from SpinnerLidar instrument, ±400 wind speed measurements plotted against SpinnerLidar internal coordinate system, Sx and Sy, wind speed measurements given in meters per second

At last, when the spherical coordinates for all the points are corrected, rotated and converted to a right-handed system, the real Cartesian coordinates of the points can be determined by,

$$\begin{aligned} y &= f * sin^{-1}(\Theta_{real}) \\ z &= f * sin^{-1}(\Phi_{real}) \\ x &= f * cos^{-1}(\Phi_{real}) * cos^{-1}(\Theta_{real}) \end{aligned} \tag{5.4}$$

Here f stands for the focus distance of the lidar instrument, which can change slightly with time. Multiplying the projection of the unit vector with the true length of the focus distance gives true measures for the locations of the measurement points.
Furthermore the axis are changed to more realistic definitions, the x-axis is defined in the direction of the looking direction of the instrument, the y-axis in the lateral direction and the z-axis in the direction of looking upwards.

To quantify the locations of the measurement in an absolute sense, the real location of the instrument has to be known. During installation the SpinnerLidar was placed on top of the nacelle so that the scanner head was at 2.9 meters above hub height (80m).

$$z_{real} = z + 82.9m \tag{5.5}$$

5.1.2 Filtering

In this campaign the SpinnerLidar was installed on top of the nacelle behind the blades, instead of in the spinner of the turbine. This practicality caused a necessity for filtering of the data before it could be handled for further research. As can be seen in Figure 5.2 in the lower region of the scanning plane, a large part of the reflections are not representing reliable wind speed measurements (dark blue color, meaning they are below 4 m/s and therefore not in the same range as the other measurements), these are measurements which are obstructed by the top of the nacelle. The laser beam is hitting the roof of the nacelle and measures an erroneous reflection because it is not moving and it is out of focus. Also over the whole scanning plane occasionally zones of erroneous measurements are visible, which are caused by the blades of the turbine passing by in front of the instrument.

Figure 5.3 shows one minute of SpinnerLidar measurements plotted against the azimuth angle of the measurement location. In this plot it can clearly be seen that there are invalid measurements over the whole plane. To correct for these faulty measurements, two criteria are being used:

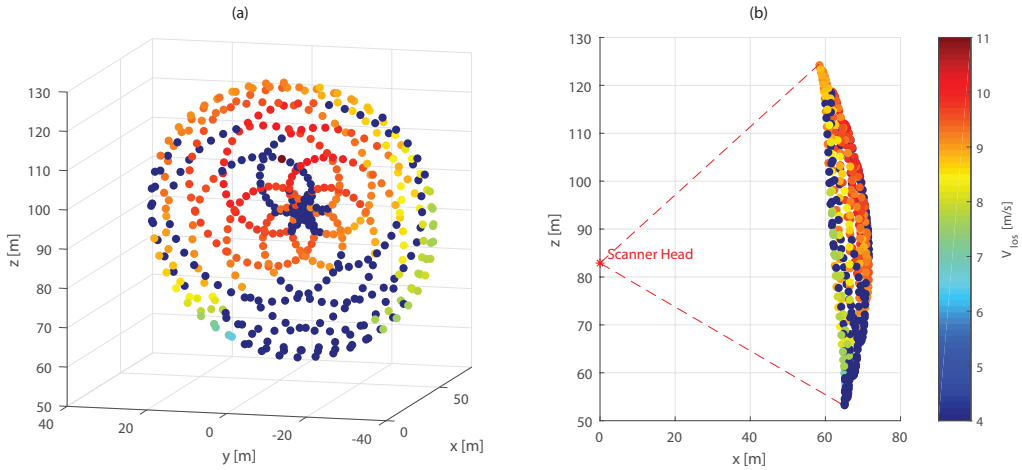

Figure 5.2: Measurement locations in real dimensions after corrections for tilt and 90 degrees rotation, (a) shows a front view from what the measurement plane will look like from a nacelle point of view, (b) shows the same measurement plane from the side with the location of the SpinnerLidar scanner head as well

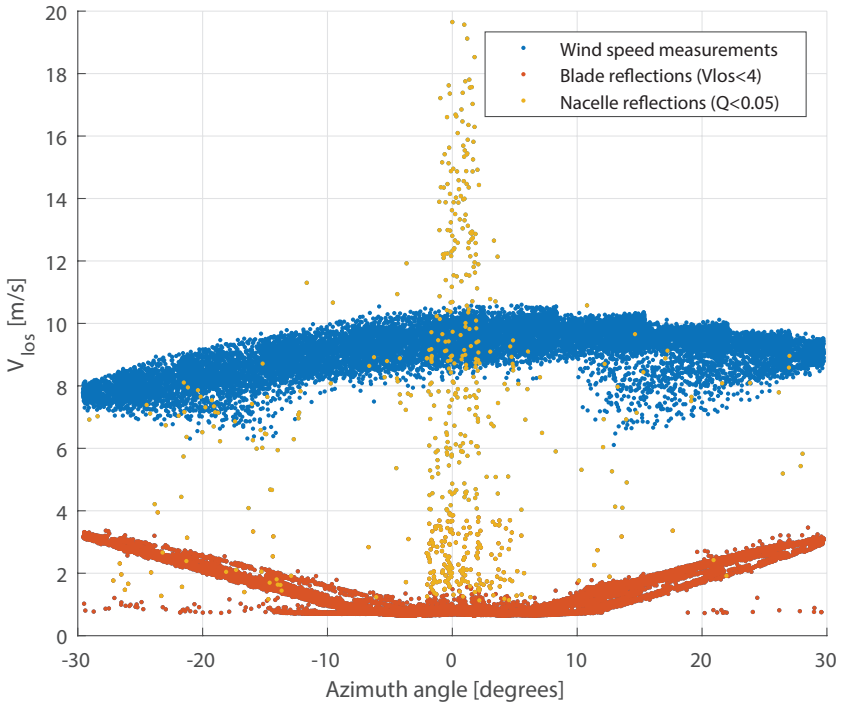

Figure 5.3: Wind speed measurements (blue) plotted against azimuth direction showing the need for two filter criteria, (red) the blade reflections, (yellow) nacelle reflections

- **Quality > 0.05**
  Quality is given in the output dataset as a quality factor for every measurements. It is determined on the basis of returned power and can thereby tell something about the measurement being in the focus range or not. Reflections from the nacelle typically have a very low quality factor as there is never a Doppler shift in these returns and the reflections are too close, resulting a low quality factor. By filtering for this factor the nacelle reflections can thereby be eliminated.

- **Vlos > 4**
  In the lower region of the plot the reflections from passing blades can be distinguished. As the blades are moving, they can cause a slight Doppler shift of the light which can be measured by the instrument. In the middle the moving direction of the blades is perpendicular to the viewing direction of the laser beam and thereby speed measurements are close to zero. But at the edges the speed measurement of the reflection of the blades can go up to about 4 m/s. It is therefore that a filtering criteria is applied for measurements up to 4 m/s, all measurements below this threshold are not considered in characterizing the incoming wind field. Luckily during this measurement campaign, average wind speeds at 80 meters were often higher than 4 m/s.

A last observation which can be made is that measurements never sink below the boundary of approximately 0.92 m/s. This occurs because lidar instrument suppress the first 5 frequency bins of the Doppler returns (Angelou and Sjöholm [2015]). But due to the higher filtering criteria as mentioned above, this becomes irrelevant.

5.1.3 Line of Sight (LoS) wind component

An important aspect about the SpinnerLidar is the incidence angle with which the instrument is measuring the movement of the aerosols. Every existing single beam lidar instrument can only measure one component of a moving object, namely the component in the direction of the beam.
Imagine the coordinate system as described above, where the x-axis is equal to the looking direction of the lidar, the y-axis is the lateral displacement in the plane and the z-axis describes the height. Every movement of an air particle in this coordinate system can be described by 3 components, u in the direction of the x-axis, v in the direction of the y-axis and w in the direction of the z-axis.

Let us assume a scenario in which the turbine, and thus the looking direction of the SpinnerLidar, is directed exactly into a homogeneous wind field.
A measurement taken at the exact middle of the viewing plane will only measure the u-component of the movement of the particle in this location. The v- and w-component can not be measured at this location as both these direction are perpendicular to the line-of-sight, and also in this scenario both these components are zero. The true speed and wind direction is therefore equal to the LoS measurement taken at this location.
Now consider a measurement taken at the edge of the plane. Due to the fact that the viewing direction is now making an angle with the x-axis, the component measured of the wind speed in the x-direction will be smaller than the true value. Also, in a case where v and w are not zero, these will also have an influence on the measured line-of-sight component of the true wind, as now the angle between the y- and z-axis and the viewing direction is not perpendicular anymore.

5.1.4 Cyclops syndrome

The problem of LoS measurements as described above is commonly referred to as the 'Cyclops syndrome' of single beam lidar instruments. Although a single Lidar can scan the line-of-sight projected wind component at multiple points upwind in front of a rotating wind turbine, it is in principle not possible to resolve all three wind components of the wind velocity vectors simultaneously from a single lidar (Mikkelsen et al. [2016]). One can compare it to looking with one eye, like a Cyclops. To be able to see depth, an extra eye, movement of the one eye or knowledge about the surroundings is needed. The Spinnerlidar is a single measuring instrument and was focused at a single distance from the turbine instead

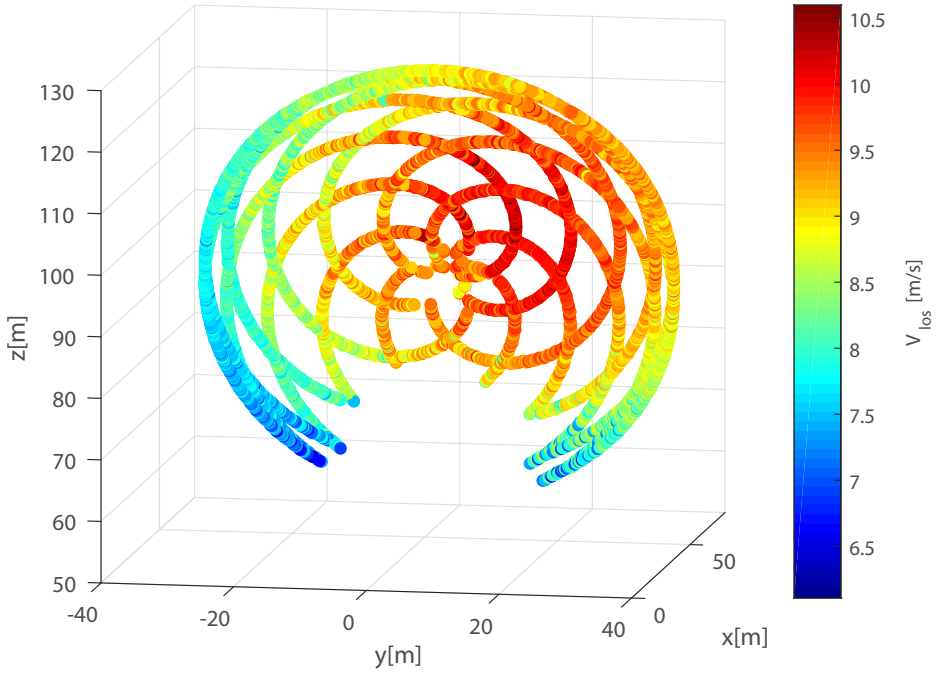

Figure 5.4: Resulting measurements of one full minute of SpinnerLidar data after filtering and location corrections have been applied

of multiple. Therefore the only way to tackle the Cyclops syndrome in this campaign is by making use of the knowledge about the incoming wind field, thus the inflow wind field.

In the example of the previous section, an ideal scenario was considered with a homogeneous wind field of which the averaged wind direction was perfectly aligned with the yawing of the wind turbine. With this knowledge about the surrounding the true wind speeds at each location could easily be determined. But as always with real-time measurements, the surroundings are never ideal.

Consider measurements of a full minute, filtered as described in the previous section, in Figure 5.4. Obviously the wind field is not homogeneous in this particular case. Therefore assumptions have to be made about the atmospheric conditions to be able to retrieve the true wind field from these measurements. There are four possible atmospheric conditions which could have caused this image of the measurements field. A short summary (also see Figure 5.5):

- **Averaged horizontal stream direction (d_h)**
  In an ideal case the averaged horizontal wind direction would always be perfectly aligned with the viewing direction of the lidar and thus the yawing of the turbine itself, obviously to catch the most wind to create as much energy as possible. However, it occurs that this is not always the case. Due to small short-term fluctuations in the wind direction or a delayed steering algorithm for the turbine a yaw misalignment is not uncommon. (see Figure 5.5a)

- **Horizontal shear (s_h)**
  The surface layer of the atmosphere can be very turbulent, in such a way that horizontal differences in wind speed can be present. The scanning plane has a lateral range of over 70 meters. Obstructions in the induction zone of the turbine (for example wake effects of other turbines) could cause fluctuations in the horizontal shear of the wind speed. (see Figure 5.5b)

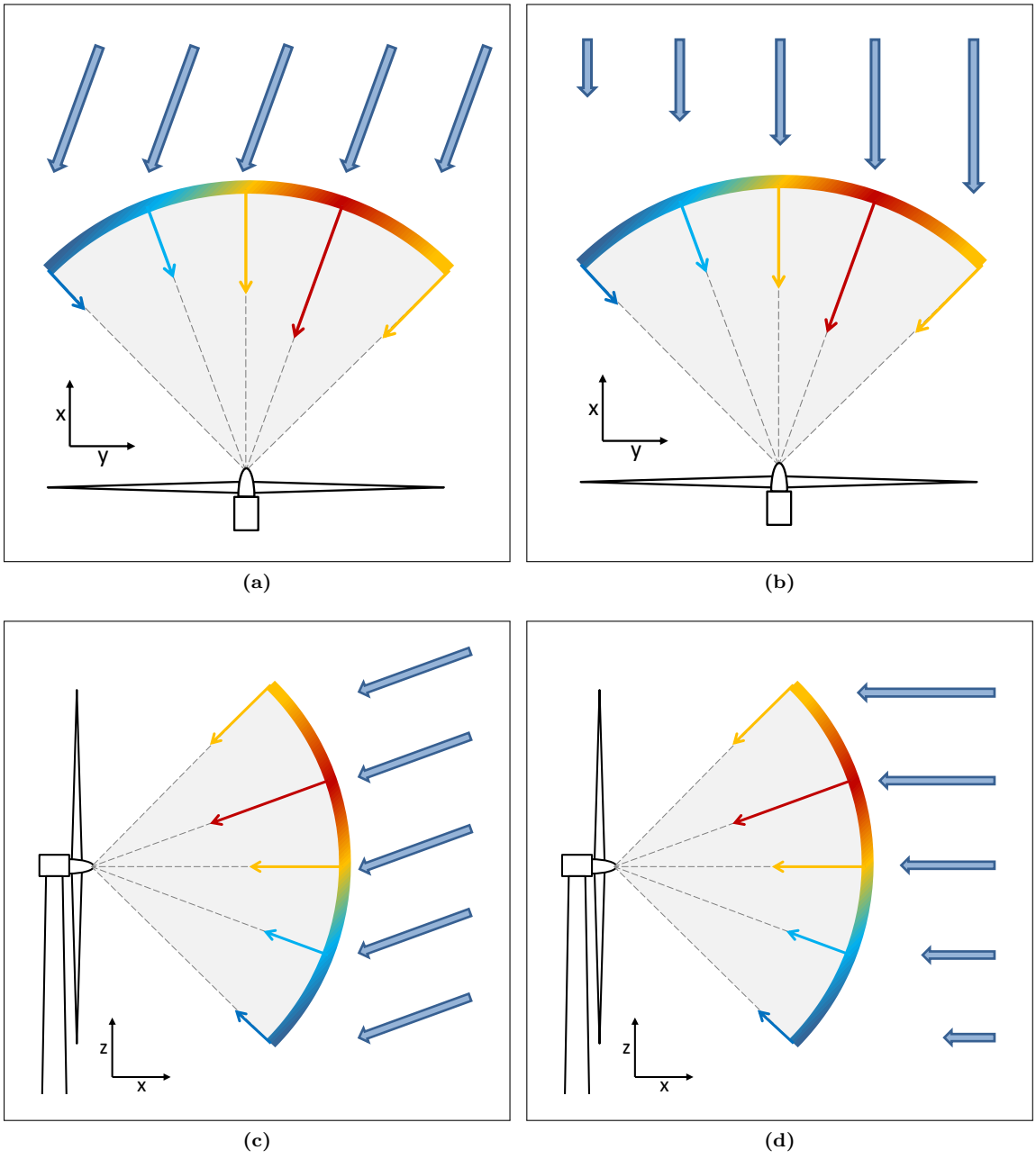

Figure 5.5: Four possible atmospheric conditions which might be the cause of a non-centered inflow:
(a) Averaged horizontal stream direction (d_h), top view of how a change in wind direction can effect the inflow measurements
(b) Horizontal shear (s_h), top view of how change in wind speeds horizontally can effect the inflow measurements
(c) Averaged vertical stream direction (d_v), side view of how vertical wind can effect the inflow measurements
(d) Vertical shear (s_v), side view of how a vertical shear in wind speeds can effect the inflow measurements

- **Averaged vertical stream direction (d_v)**
  In hilly terrain an averaged vertical wind component is certainly not uncommon. But also in flat terrain, at daytime when there is heating of the sun, the w-component of the wind can be non zero. (see Figure 5.5c)
- **Vertical shear (s_v)**
  Standard atmospheric law tells us that the boundary layer always follows a vertical shear in wind speed. Power law or logarithmic, the wind speed is increasing with height, due to the fact that the wind in the lower regions is experiencing more friction of the surface than in upper regions. Such a shear is typically stronger during nighttime when there is no incoming solar radiation to cause mixing in the boundary layer. (see Figure 5.5d)

5.1.5 Free inflow assumptions

All four atmospheric conditions as described above could, in a combination, lead to the measured pattern as shown in Figure 5.4. But making a distinction between the two horizontal and vertical factors seems impossible without further knowledge. In this research therefore only the moments of free inflow during the measuring campaign are used for further validation and characterization of the wind field. In free inflow conditions, so when no obstacles are influencing the inflow wind field of the turbine, two assumptions can be made about the atmospheric conditions.
One is in the horizontal direction. Namely that it is unlikely, with no obstacles influencing the wind field, that there would be a horizontal shear or difference on the scale of 70 meters over the measuring plane. Therefore the only remaining option to cause a shift in the lateral direction would be a misalignment of the viewing direction of the lidar with respect to the averaged horizontal stream direction, which is very likely.
The second is an assumption in the vertical way. In free inflow it is more likely that a vertical shear is dominating the wind profile more than a possible vertical wind component. Certainly during night hours the free inflow wind field should be partially laminar and there will be almost no wind movement in the vertical direction.
In this way the two factors influencing the wind field can also be seen as independent to one another. Correcting for one of these phenomena will not influence the magnitude of the other.

This proposed method is relatively simple, but very efficient if applied to only free inflow data of this measurement campaign. When the inflow wind field is not from an open space and may thus be including wakes or other disturbances, the two assumptions as described above will not hold. Luckily during the span of the ScanFlow measurement campaign, the periods of free inflow for this particular turbine were sufficient for further research. As described in the previous chapter the turbine R9 is the most Easterly located turbine of the EWTW test site facility. To the East of this turbine there are no large obstacles which could cause obstruction of the incoming wind field. It can be determined from site plans of EWTW that when the turbine has a yawing direction between 2.4 and 167.6 degrees (North) the inflow wind field should not contain any wakes of nearby turbines. A benefit of measuring in the winter months is that next to the main wind-direction from the South-West for this location, the wind is more likely to come from the East as well in this period of the year.

5.1.6 Determination of processing period

The independent assumptions about the inflow wind field, the misalignment of the horizontal wind direction and the vertical shear, can be applied to any period of SpinnerLidar data. However, as will follow in the next session, there are certain requirements for the amount of data which is needed to correct for these assumptions.

Finding the true horizontal wind direction from the measurements will turn out to be crucial for successful transformation of the LoS measurements. But to make a good estimation of this wind direction, the processing period is important. If the processing period is too short, say a few seconds, there will be only

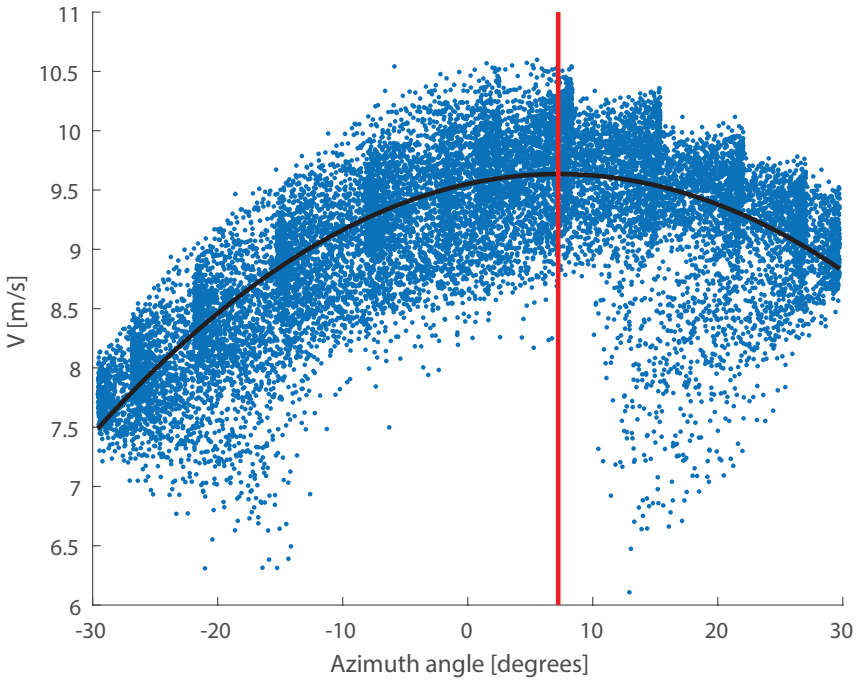

Figure 5.6: Filtered wind speed measurements (blue) plotted against azimuth direction, the black line is a 2nd degree polynomial least-square fit of all the measurements, the red line indicates the maximum of this fit and thereby also the estimated angle of where wind speed measurements are the highest, which would indicate that the wind is coming from this direction

little wind speeds measurements to accurately determine the wind direction. If the processing period is too long, say 10 minutes, there will be enough data, but during a period of 10 minutes the wind direction can also change, making it too averaged. Therefore a processing period of 1 minute was chosen to use in transforming the LoS wind speed measurements.

5.1.7 Processing algorithm

The first characteristic that can and has to be obtained from the data is the averaged horizontal stream direction. If the vertical differences in wind speed are disregarded, and the wind speed measurements of 1 minute are plotted against the azimuth angle (Θ_{real}), the averaged horizontal stream direction of this period can be found by localizing the averaged maximum of this plot. This is namely the place where the laser beam direction is colliding head on with the direction of the moving aerosols, thus measuring the largest component. It was assumed that horizontal shear is absent so this maximum can only be caused by a mismatch between the looking direction of the turbine and the averaged horizontal stream direction. The angle found by this approach is the direction the turbine should actually have been facing to capture the most energy from the wind.

Figure 5.6 shows an example of one minute of SpinnerLidar data plotted against the azimuth angle. To find the maximum to this plot a simple 2nd degree polynomial was used to best fit the data in a least-squares sense. Next the maximum of this fit in the range of the measurement plane is determined. If the maximum of the fit lies at the edge of the measurement plane the located maximum is considered as unreliable, as it might be the case that the true wind direction angle lies beyond the range of the measurement plane. Therefore the particular minute is disregarded as a good measurement.

Important to notice is that the averaged horizontal stream direction found by this approach is, as the name says, averaged over the whole vertical distance. Theory suggests that wind veering, the turning of

wind direction with height, can be present in a wind profile over this range (Wallace and Hobbs [2006]). The presence of more data in the upper regions than in the lower regions of the plane in combination with possible wind veering tends to lead to an overestimated angle of averaged horizontal stream direction. For that case the averaged horizontal stream direction for the whole plane was determined by looking only at the measurements around hub height, between 70 and 95 meters. The phenomenon of wind veering and its effect on the data and this proposed method will be further discussed in Chapter 8.

The averaged horizontal stream direction together with the assumption that the averaged vertical stream direction is zero can form a general direction vector for the wind direction over the whole plan. Every single line-of-sight measurement can then be considered as a component measurement of this general direction vector. Using the laws of vector projection this leads the following formula:

$$\vec{V_{los}} = \begin{bmatrix} \Theta_{real} \\ \Phi_{real} \\ f \end{bmatrix}, \quad \vec{d_h} = \begin{bmatrix} \Theta_{max} \\ 0 \\ f \end{bmatrix} \tag{5.6}$$

$$\hat{V_{los}} = \frac{\vec{V_{los}}}{||\vec{V_{los}}||}, \quad \hat{d_h} = \frac{\vec{d_h}}{||\vec{d_h}||} \tag{5.7}$$

$$V = \frac{V_{los}}{\hat{V_{los}} \bullet \hat{d_h}} \tag{5.8}$$

The line-of-sight direction can be stated for every point as a vector of Θ_{real}, Φ_{real} and f. The averaged horizontal wind direction vector is given by $\vec{d_h}$. Dividing the LoS measurement at each location by the dot product of the normalized direction vectors, gives the original magnitude of the true wind speed in the direction of the averaged horizontal wind direction, of which the LoS measurement was only a component.

The applied correction for every measurement should give the true magnitude of the wind speed at every location instead of the LoS component, and should thereby correct for the Cyclops syndrome. Figure 5.7 shows an example of the applied method. It can be seen that the newly calculated wind speeds show a far better representation of the true wind field than the original measurements. The spherical structure, caused by the increasing incidence angle of the measurements towards the edge, is not visible anymore. The differences in the lateral displacement are very small, while the only recognizable pattern remaining is the vertical shear, which is to be expected in measuring a wind profile.
With the lateral displacement being small, a next step in the process of defining wind characteristics is determining averaged wind speeds at certain height levels. The corrected measurements (V) at a 10 meter interval around fixed heights of 50, 60, 70, 80, 90, 100, 110 and 120 meters are averaged. These intervals are the same as the programmed intervals for the WindCube. The standard deviation at each height level gives a good measure for the uncertainty of the calculated average value.

5.1.8 Determination of sample size for cross-validation

As stated before the selected epoch to process the data of the SpinnerLidar was chosen to be 1 minute, meaning 1 minute characteristics are being retrieved from the above mentioned approach. This, however, is not a standard epoch to use in wind profiling research. 10 minute interval characteristics are much more common as is shown by the output of the WindCube which has a temporal resolution of 10 minutes.

In order to compare the retrieved SpinnerLidar wind characteristics to the WindCube measurements the epoch had to be changed. The processed minutes of available SpinnerLidar data were selected on the basis of if this certain minute was receiving free inflow or not. But for the transition to 10 minute characteristics this selection criteria was restricted so that a series of 10 consecutive minutes all have to receive free inflow before it can be compared to data of the WindCube. Of course it is not completely certain that the WindCube would also receive full free inflow during this 10 minute period, but this small uncertainty will have no large consequences as the WindCube still averages its data over the span of

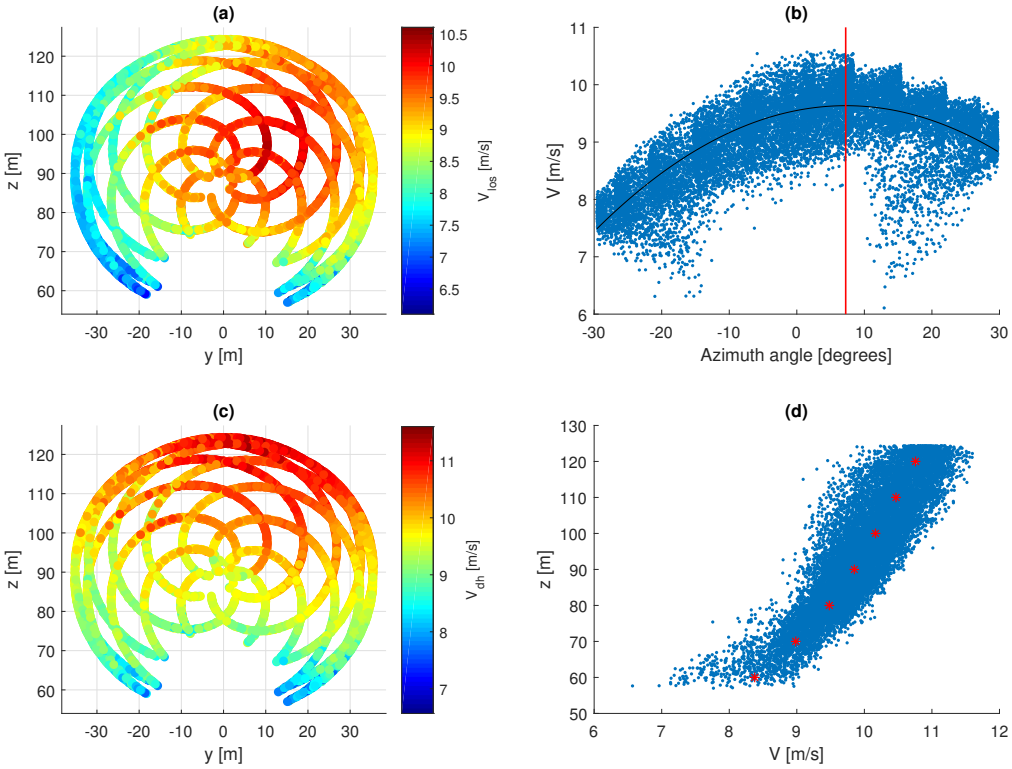

Figure 5.7: Full processing algorithm for 1 minute of SpinnerLidar data:
(a) Filtered measurement data plotted against corrected location
(b) Filtered measurement data plotted against azimuth to find averaged horizontal wind direction with a least-square fit
(c) Projected and transformed measurements on averaged horizontal wind direction
(d) Transformed wind speed measurements plotted against height

10 minutes. Still, after applying this harsh selection criteria, more than a thousand 10-minute periods remained over the whole campaign in which free inflow over the whole 10 minutes was guaranteed with a high enough average wind speed to be able to filter correctly.
The methods of correcting the measurements from LoS to their true magnitude stays the same, and is still done on a 1 minute basis. But after this processing the 10 values for a 10 minute period are combined into an averaged value for this period to compare to other instruments like the WindCube. For example, 10 consecutive processed minutes of the SpinnerLidar data from time-stamp "20:10 01-02 2017" till "20:19 01-02 2017" are combined to one 10 minute period time-stamp, to be compared to the WindCube measurement of "20:10 01-02 2017", as the WindCube is programmed to give the first minute as a time-stamp to every following 10 minute period.

5.2 WindCube Data

The data in the output file of the WindCube is almost immediately suitable for comparison. Where the SpinnerLidar data is very raw and needs lots of corrections to find the true wind speeds, the WindCube has internal algorithms and therefore outputs true wind speeds instead of LoS measurements.

The WindCube is, just like the SpinnerLidar, scanning in a conical pattern to measure the wind speed and direction. It is a pulsed lidar so the returns are binned by predefined height intervals to obtain wind speed measurements at certain heights. These measurements are also line-of-sight measurements at first. Inside the instrument predefined algorithms convert these LoS measurements to averaged wind speed and direction measurements for the selected height over an interval of 10 minutes.

The standard deviation for the horizontal and vertical wind speeds are also determined by the instrument over each 10 min period. But these measurements and standard deviation of vertical wind speeds are not used in this research, because for correcting the SpinnerLidar data the assumption was made that there would be no vertical movement of the air particles in free inflow. After averaging the vertical wind component as measured by the WindCube in the periods of free inflow, this value indeed turned out to be close to zero.

5.2.1 Filtering

The WindCube also determines a quality factor, called the Data Availability for each measurement taken, depending on the Carrier-to-Noise-Ratio of the returned signals. This parameter ranges from a value of 0 to 100 percent. It was chosen to use a threshold of 75 (meaning the returned signal having 75% of the expected power), to filter the erroneous measurements from the data. As the WindCube data is only used for validation purposes in this research, only the data in the same epochs as when the SpinnerLidar was obtaining free inflow are used to compare.

CHAPTER 6

Validation of SpinnerLidar data

The method configured and described in the previous chapter was used to handle the data of the SpinnerLidar and WindCube in such a way that the measurements can be compared. Validation of especially the SpinnerLidar data is needed to be able to use this data to correctly characterize the inflow wind field.

6.1 Validation against WindCube

The corrected SpinnerLidar measurements are validated against the measurements from the WindCube. Comparing two lidar instruments might not be ideal, because of the slightly higher inaccuracy of lidar instruments than for example cup anemometers. However, the WindCube is one of the lidar instruments which has experienced a rapid increase in usage over the past years and is starting to become a well-known, trusted wind profiling instrument.
Another reason to choose for a validation of the SpinnerLidar data using the WindCube is the fact that the meteo-mast, from which the data was also collected during the campaign, is located much further away from test turbine R9 and in the wrong orientation. As told before only the free inflow periods of the SpinnerLidar data will be used in this research, to make certain the assumptions about the incoming wind field (needed for correcting the Cyclops syndrome) will hold. These free inflow criteria required Easterly wind. The meteo-mast is located to the South-East of turbine R5 (the most Westerly located test turbine). Therefore the meteo-mast will experience disturbances from the wakes of all the test turbines in cases of wind coming from the East. The wind measurements of the meteo-mast can therefore not be regarded as absolute free inflow measurements in times when the SpinnerLidar is retrieving free inflow.

6.2 Wind direction at hub height

The first criterion used in the method to correct for the Cyclops syndrome is the averaged horizontal wind direction. This value is determined on the basis of the raw LoS measurements of the SpinnerLidar and therefore makes a good parameter to validate first in order to create a solid basis on which the rest of the corrections are done.
The averaged horizontal wind direction was determined around the lidar height (82.90 meters), by only using the measurements between a height of 75 and 90 meters. The estimated value of averaged horizontal

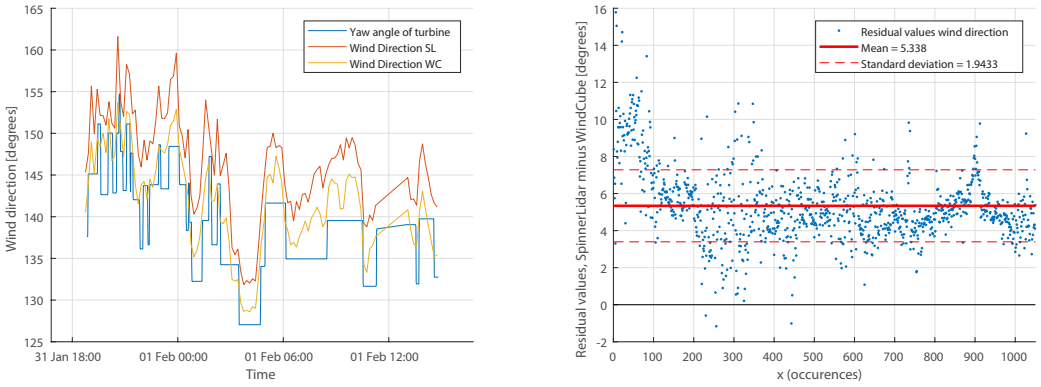

(a) **(b)**

Figure 6.1: Comparison of horizontal wind direction as measured by the SpinnerLidar (SL) and WindCube (WC), (a) shows the measured wind directions over a brief period, (b) shows the difference in measured wind direction over the whole campaign for the SpinnerLidar and WindCube together with the calculated average offset and standard deviation

wind direction is at first a value in the internal coordinate system of the SpinnerLidar, a value in the range of azimuth angles of the measurement locations. To make this averaged horizontal stream direction absolute, the known direction of the turbine with respect the North had to be added. As of this conversion to real world wind direction is was first assumed that the SpinnerLidar was perfectly aligned with the viewing direction of the wind turbine. The WindCube determines the horizontal wind direction at every 10 meter interval, so for this comparison the closest 10 meter interval at a height of 80 meters is used.

Figure 6.1a shows for a brief period the yawing angle of the turbine, the wind direction as measured by the WindCube and the calculated wind direction as measured by the SpinnerLidar. Immediately it can be seen that both instrument show a very coherent pattern. However, the wind direction as measured by the SpinnerLidar has a bias in regards to the measurements of the WindCube. The wind direction as measured by the WindCube correlates much better to the yawing direction of the turbine, suggesting the WindCube is doing a better job.

There is however a quite simple explanation for this offset. As can be seen in Figure 6.1b the offset of difference in measured wind direction is quite constant over the span of the campaign. The averaged offset is 5.338 degrees with a standard deviation of just below 2 degrees. This constant offset suggests that it is likely that there might be some sort of instrumental error in one of the machines, most likely the SpinnerLidar as this one is deviating more from the yawing of the turbine. A very likely explanation could therefore be an inaccurate installation of the SpinnerLidar on top of the nacelle. In the horizontal wind direction detection method it was assumed that the SpinnerLidar is perfectly aligned with the viewing direction of the turbine. But if the SpinnerLidar is not installed properly and is viewing slightly to the left of the viewing direction of the turbine, the maximum wind speeds and therefore wind direction will always lay in the right part of the measurement plane. After reviewing the installation procedure as executed by ECN, an installation error was determined to be very likely.

Despite this detected offset the correlation between the two instruments remains very high. The offset does not infect the processing algorithm itself but only the conversion of the locations of the measurement to real dimensions. For the further characterization of the inflow wind this has no effect. The confirmation that the procedure for retrieving the averaged horizontal wind direction from the SpinnerLidar is correct, is important for the rest of the research in which wind speeds are calculated using this averaged horizontal wind direction.

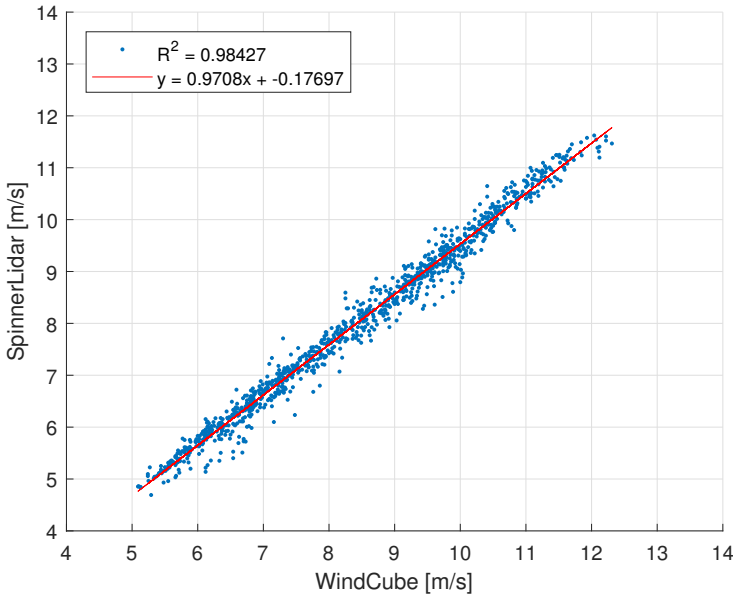

Figure 6.2: Compare wind speed at 80 meters

6.3 Wind speed at hub height

Evidently the validation of the the wind speed measurements of the SpinnerLidar says much more about the usefulness of the instrument than the validation of the measured averaged horizontal wind direction. In Chapter 5 it was described how the LoS wind speed measurements are converted to real wind speeds and how all these wind speeds could be averaged to a wind speed profile.
Every averaged wind speed measurement at a specific height from the SpinnerLidar data can be compared to the averaged wind speed measurement at the same height during the same 10 minute period from the WindCube data by a regression analysis. This would give a regression analysis plot for each height level (seven in total). In Figure 6.2 this plot at a height of 80 meters is displayed, 80 meters being the closest to hub height. The averaged horizontal wind direction was determined with the measurement around hub height, meaning the conversion from LoS to real wind speed values should be the most accurate around hub height. Further away from hub height wind veering could have its effect on the validity of the conversions. The regression analysis plots for the other height levels are given in Appendix D

The correlation at 80 meters between the two instruments is very high indicated by the R^2 value of 0.98. Also at other heights levels the correlation is always above 0.97, meaning that the wind speeds as measured and transformed by the SpinnerLidar are in very good agreement with the wind speed measurements of the WindCube. When comparing the regression analysis plots for all height levels the observation can be made that they almost all indicate an offset of around -0.2 m/s between the SpinnerLidar and the WindCube, meaning the SpinnerLidar is constantly measuring a slightly lower wind speed than the WindCube at the same moments in time. On top of that the slope of the correlation fit is slightly below 1, which would mean that with higher wind speeds, the offset between the two instruments becomes larger. Possible explanations for this observation could lay in something called the blockage effects of a rotating turbine or maybe small calibration errors, but this will be further discussed in Chapter 8.

Overall it can be said that the SpinnerLidar is showing very similar results for mean wind speeds with regard to the WindCube, which itself, as showed in Chapter 2, has been validated multiple times against well-known wind profiling instruments. It is therefore believed that the method applied to the Spinner-Lidar data to correct for the Cyclops syndrome in free inflow, as proposed in the previous chapter, is working very well.

CHAPTER 7

Characterization of turbine inflow

For validation purposes the measurement data of the SpinnerLidar had to be generalized in multiple ways to be able to compare it to the WindCube measurements. The temporal resolution was decreased to match the 10 minute sampling rate of the WindCube, but in particular in a spatial sense enormous amounts of data had to be disregarded.

The validation was very successful, as showed in Chapter 6, meaning the suggested algorithm is working. But due to the lower sampling rate of the WindCube this validation is officially only proved for average wind characteristics. This seems to be a reoccurring problem in wind lidar research as in Chapter 3 it was also indicated that validating turbulence measurements from lidar systems is yet to be done. However, previously the argument was made that a validation of the mean wind characteristics can help in making turbulence research from lidar systems more certain by ensuring the mean wind characteristics measurements are reliable.

The remaining data of the SpinnerLidar contains such a vast amount of information about the inflow wind field, that it can in no way be compared to results of previous studies in this research field. It leads to an unique opportunity to study the inflow field with a very high temporal and spatial resolution. But because there is no accepted method to process this kind of data yet, the following work may be considered as a pioneering study.

7.1 Quantifying individual measurements

The vast amount of data is clearly visible in Figure 5.4, where only 1 minute of data is plotted in the measurement plane. All these single measurements tell something about the incoming wind field but can not all be considered independently.
To be able to tell something about all these measurements a method is proposed to create an overview of the inflow wind field.

7.1.1 Grid boxes, mean and turbulent intensity

The whole measurement plane can be divided in grid boxes in such a way that all the individual measurements can be assigned to one of these grid boxes. In this case a resolution of 5 by 5 meter was applied. The reason to choose for this grid structure originates in Chapter 4 where it was explained that

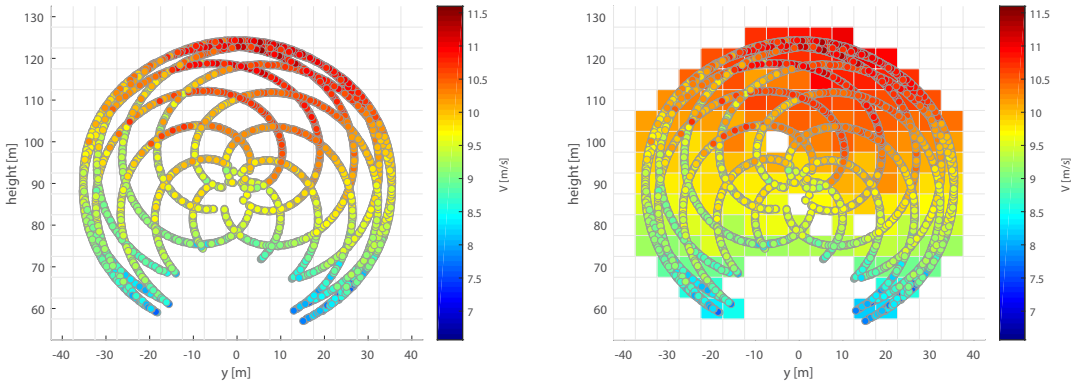

Figure 7.1: Example of grid applied to individual measurements, (a) SpinnerLidar data of 10 minutes superimposed on grid of 5 by 5 meters, (b) mean wind speeds values calculated for every grid cell by using all individual measurements within one grid cell

the location of the measurements of the SpinnerLidar is never exactly the same for every reoccurring second but shifts a bit due to the sampling rate of 400.2305328 Hz. By making grid boxes of 5 by 5 meter over the whole plane, and capturing all measurements of a full minute in this grid, the inaccuracy of the timing and location of measurements becomes less relevant. Figure 7.1 shows an example of the applied grid.

Subsequently all the measurements within one grid box could be combined to calculate an average wind speed value for each box, but also to determine the variance of wind speeds measurements. The mean wind speed values per box will give an indication for the wind variety in the vertical but also horizontal direction. The variance of wind speeds in every cell is calculated as follows:

$$\sigma_u = \sqrt{\frac{1}{N}\sum_{i=1}^{N}(u_i - \bar{u})^2} \tag{7.1}$$

Here $\bar{u}$ symbols the average (horizontal) wind speed as calculated in one grid box. The variance of wind speeds can be used tell something more interesting about the inflow wind field. Namely that with the use of this variance and the mean wind speed the turbulence intensity, as already described in Chapter 2, can be calculated.

7.1.2 Time interval

The time interval over which the measurements are combined in the grid cells can be adjusted. It would make sense to calculate the mean wind speed and variance per grid box over a period of 1 minute, the same period which was used to correct the LoS measurements. But the 10 minute period, as used for the validation, is also a well known time scale in wind research, which could be better compared to other studies and to the data of the WindCube. Therefore a period of 10 minutes was chosen, which means all individual measurement of a full 10 minute period are divided over the grid boxes and used to calculate the previously mentioned 10 minute wind characteristics for every grid box over the whole measurement plane.

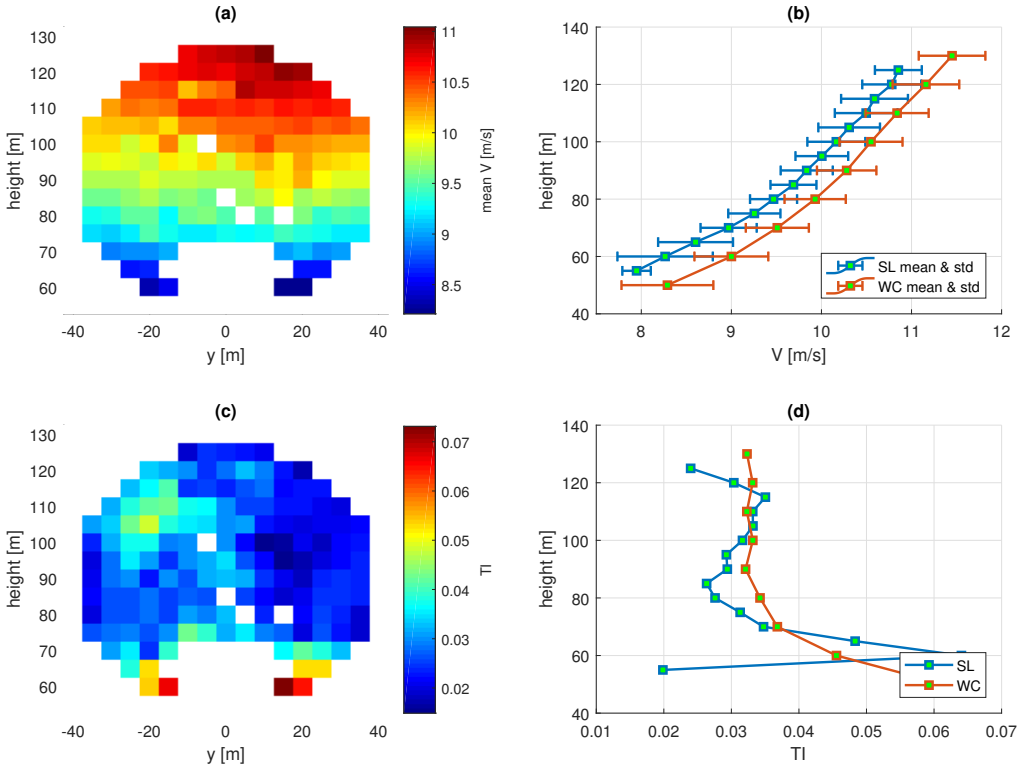

Figure 7.2: Example of characterization of inflow wind field of one 10 minute period (1st February 2017 20:17)

7.1.3 WindCube profile validation

Using a 10 minute period makes it possible to compare the results of this characterization with the WindCube. The whole profile in intervals of 5 meters can easily be determined in the same way that the average value per grid box was determined. Instead of separating in the lateral distance, now all measurement of one specific 5 meter height band will be combined to an average wind speed value per height level. Again the standard deviation of this averaged value can be computed. This extra comparison of the (transformed) measurements of the SpinnerLidar against the measurements of the WindCube for every 10 minute period gives a good sense for how valid the values for wind characteristics are. This gives the assumptions based on these characteristics more credibility. See Figure 7.2b for an example.

Not only the average wind speeds profiles can be compared, but also the turbulence intensity profiles of both the SpinnerLidar and WindCube. For the SpinnerLidar the values of turbulence intensity of each grid box are combined in a lateral sense to calculate an average value for each height level. For the WindCube the given standard deviation at each height level is divided by the mean wind speed at this level to obtain the turbulence intensity. Both these profiles can than be plotted next to each other, see Figure 7.2d.

7.1.4 Visualization of characteristics

Figure 7.2 gives an example of the proposed characterization method for one single 10 minute period during the ScanFlow campaign (1st February 2017 20:17). As can be seen all the grid boxes which include some measurements have been given a value for the mean wind speed and turbulence intensity in Figure 7.2a and 7.2c. Some boxes are left empty as they contained too few measurements (less than 10). In this example the averaged wind speed values show a gradual increase of wind speed over height and

have almost no significant variations in the lateral direction. Taking a look at the turbulence intensity per box, it is shown that there seems to be more variance in the lower regions of the measurement plane than higher up. This could be considered logical if one would take into account the effect of surface friction on the fluctuations in wind speed. Also there is a notable spot of higher turbulence in the upper left corner for this particular minute of data.

The comparison of the two wind profiles (Figure 7.2b) as measured by the SpinnerLidar and the WindCube show a similar gradient over height. However the WindCube seems to be measuring slightly higher wind speeds than the SpinnerLidar in this particular 10 minute period. The profiles of turbulence intensity (Figure 7.2d) are also showing the same results, with higher turbulence in the lower regions. It has to be noted that these profiles are only based on one 10 minute period and can therefore be influenced by outliers.

7.2 Classification by average wind speed

Classifying the 10 minute periods of the whole campaign can help to give inside in specific atmospheric conditions. All 10 minute periods can be classified on the base of their average wind speed. In this way a general understanding of the mean wind speed values over the measurement plane could be obtained, together with a general wind profile and turbulence intensity profile for every wind speed class. In this way figures about the wind characteristics can be obtained of every wind speed class ranging from a rounded average wind speed of 5 to 12 m/s. Figure 7.3 shows the averaged figures for the 9 and 10 m/s classes, meaning for the class of Figure 7.3b all periods with an averaged wind speed between 9.5 and 10.5 as measured by the SpinnerLidar are combined. In these classification figures the same plots as in Figure 7.2 are shown. The figures for the other classes are added in Appendix E.

A first observation which can be made is in the grid box mean wind speeds plots, in Figure A of each class. A gradual increase of wind speed with height is shown but more important, higher wind speeds in the upright corner in all classes. This could be a result of the non-corrected wind veering.

When regarding the mean wind speed profiles as seen in Figure B, the SpinnerLidar and WindCube always seem to show the same trend. However, in all cases the WindCube seems to be measuring slightly higher wind speeds than the SpinnerLidar, and it is doing so by a constant offset of about 0.5 m/s. Previously in Chapter 6 an offset of 0.2 m/s between the SpinnerLidar and WindCube has already been noted. Possible explanations can be the blockage effect of the turbine or instrumental differences, this will be further discussed in Chapter 8. Another observation regarding the wind profiles of each class show that with increasing average wind speed the vertical shear also increases, considered logical as surface friction weighs heavier with higher wind speeds. Also in the wind profiles a small deviation between the SpinnerLidar and WindCube can be observed in the higher regions, which might also point to the non-corrected wind veering.

The grid box turbulence intensity plots as shown in Figure C of each class indicate higher turbulence in the lower regions of the plane, which is confirmed when looking at the turbulence intensity profiles in Figure D, which shows the same trend over all classes. The turbulence intensity profiles of the SpinnerLidar and WindCube seem to show the same trend in most classes. In the top of the profile they tend to deviate a bit as the SpinnerLidar is measuring slightly higher values than the WindCube, in the lower regions they both go up in turbulence intensity. The averaged turbulence intensity over the whole profile for each class seems to stay about the same, from which it can be concluded that the turbulence intensity is independent of the average wind speed.

7.3 Turbulence Intensity

As mentioned above the calculated turbulence intensity is a turbulent measure independent of the magnitude of the wind speed. Therefore this measure makes it possible to average the spatial data over the whole measurement campaign regardless of inflow conditions. Still the turbulence intensity per grid box

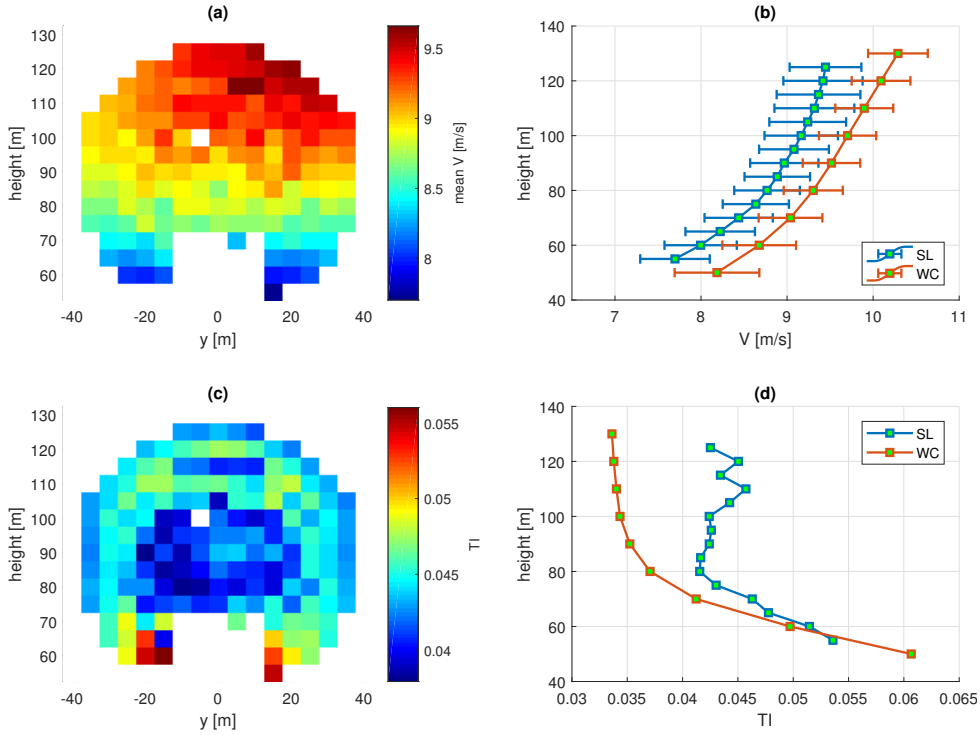

(a) 9 m/s class

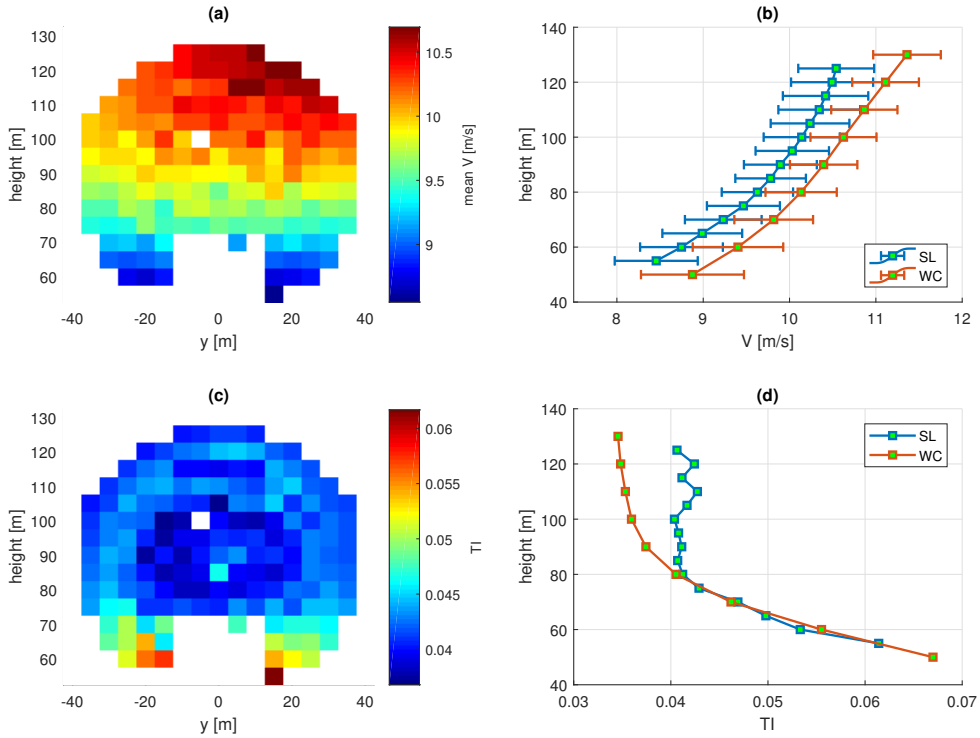

(b) 10 m/s class

Figure 7.3: (a) 9 m/s class with 117 periods, (b) 10 m/s class with 177 periods, for all other classes, see Appendix E. Within one figure: (a) mean wind speeds per grid box, (b) mean wind speed profile from SpinnerLidar (SL) and WindCube (WC) with error-bars indicating standard deviation, (c) mean turbulence intensity per grid box, (d) mean turbulence intensity profile from SpinnerLidar (SL) and WindCube (WC)

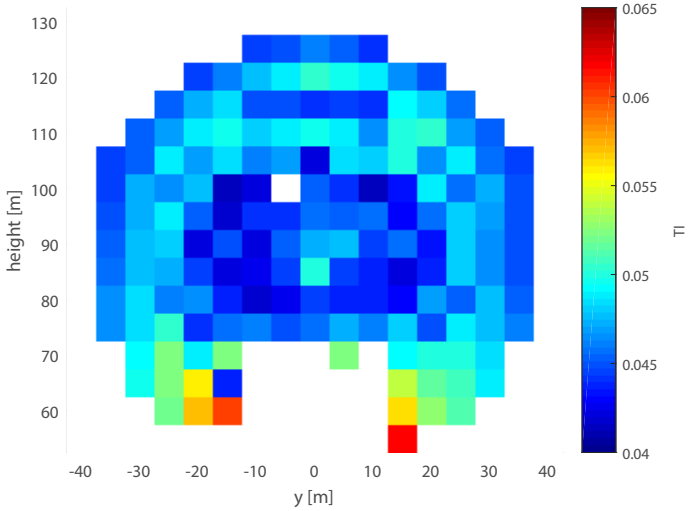

Figure 7.4: 10 minute turbulence intensity combined over all periods of free inflow conditions calculated and visualized for every grid box

is determined on a 10 minute base, but after dividing by the mean value this quantity can easily be averaged over a longer period.

Figure 7.4 shows the turbulence intensity plot of all 10 minute periods of free inflow conditions. As can be seen there still is the most variability in the lower regions of the measurements plane. The averaged magnitude of the turbulence intensity is in the same order as the results represented by Sathe et al. [2015] and Bot [2014] in earlier lidar turbulence intensity studies. However, the values as measured in this campaign are some what lower than in for example Bot [2014], but this can be explained by the fact that this campaign was executed in winter times, when turbulence is limited because of low incoming solar radiation, whereas Bot [2014] was executed in the month June when solar radiation and therefore turbulence is high.

As before, the turbulence intensity data of the SpinnerLidar can be compared against the turbulence intensity data of the WindCube in a regression analysis as shown in Figure 7.5. For this the SpinnerLidar data was binned at 10 meter intervals to match the height levels of the WindCube. The two instruments seem to show some correlation but there is definitely some inaccuracy present as the R^2 value is relatively low. Compared to other turbulent intensity studies the results are in the same magnitude for the relatively low mean wind speeds of this measurement campaign.
A last observation which could be made from the regression analysis comes forward when the turbulence intensity measures of the different height levels are separated. The colored dots show the mean values for all the turbulence intensity measurements at a specific height. It can be seen that the two lowest height levels correspond to higher TI values than the higher height levels. The same trend was already shown in the results based on Figure 7.3 and 7.4

7.3.1 Day and night difference in turbulence intensity

One of the phenomena expected to have its effect on the inflow wind field is the day-night rhythm which influence the stability of the boundary layer. At day time, the incoming solar radiation heats up the land surface in front of the turbine and causes an upward flux of energy. This flux causes turbulence in the lower profile of the boundary layer and might be visible in the scanned profile of the SpinnerLidar by a higher turbulence intensity. At night times there is no incoming solar radiation meaning the wind profile should be much more stable than at day time.

To search for this diversion all periods between 8am and 6pm were marked as day time, and the periods

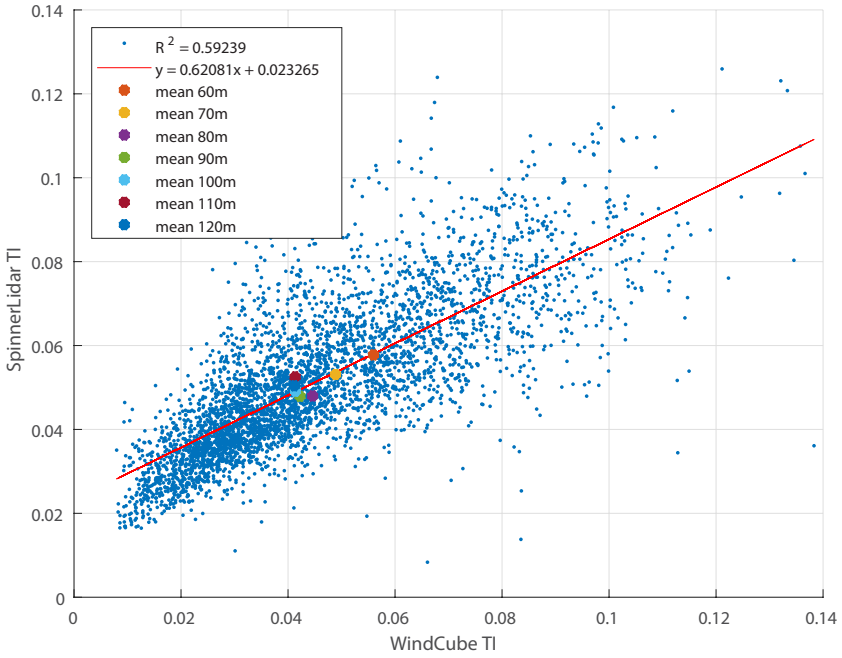

Figure 7.5: Regression Analysis of WindCube and SpinnerLidar TI data (blue). Linear fit is given (red) together with R^2 value for the regression analysis. The colored dots indicate the mean TI values of the different height clusters.

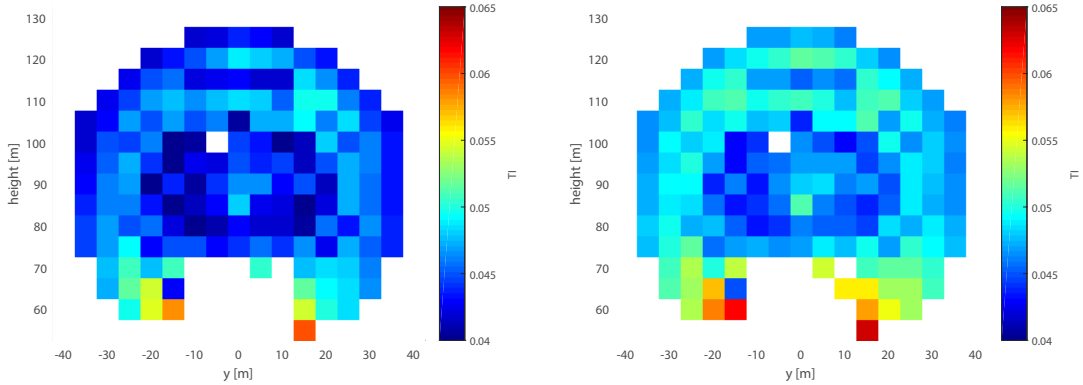

Figure 7.6: Turbulence intensity grid box plots day and night difference of SpinnerLidar data, (a) containing all day time periods between 8am and 6 pm, (b) containing all night time periods between 6pm and 8am

between 6pm and 8am as night time. Then again all 10 minute periods of turbulent intensity were combined into one plot to search for typical turbulent structures in these two separate periods. Figure 7.6 shows the result of this separation, but as can be seen a clear difference stays out. Figure 7.7 shows the same results, but then plotted as profiles, so that in this plot also the WindCube turbulence intensity profiles could be compared. The results shown are a bit contradicting as the nightly hours have a slightly higher turbulence intensity where one would expect the day time to be more turbulent. An explanation of the absence of the day and night difference could lie in the fact that the ScanFlow campaign was conducted in the winter. In these months the solar radiation is so low that it may not have much effect on the turbulent profile of the boundary layer.

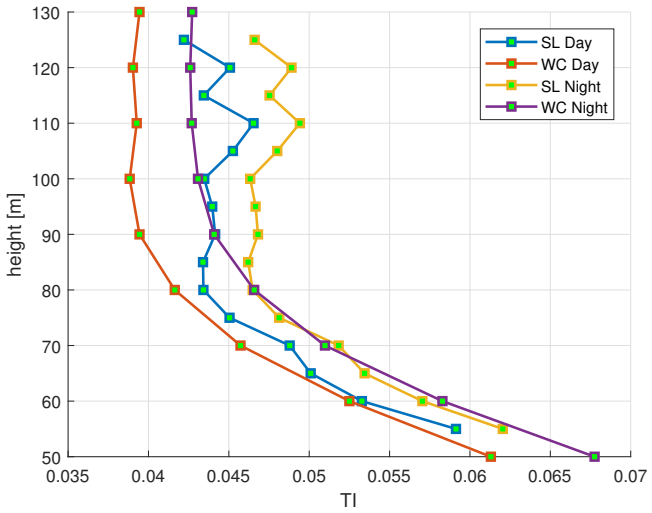

Figure 7.7: Turbulence intensity profiles separated for day and night time for both the SpinnerLidar (SL) and WindCube (WC)

CHAPTER 8

Discussion

8.1 Accuracy of wind lidar instruments in general

A returning factor of doubt in wind lidar research remains the location accuracy of the measurement instruments. As pointed out before, Sathe et al. [2015] conducted a report about several studies comparing lidar wind measurements against in-situ wind measurements from meteo masts. They concluded rightfully that when studying the micro-scale turbulent structures, lidar instruments are always prone to their probe volume. Lidar measurements are almost never taken at the exact same location meaning that averaging over this probe volume will always filter out the smaller turbulent structures. And these smaller turbulent structures also very interesting for wind energy research

In this research we compare two lidar instruments, the continuous-wave SpinnerLidar and the pulsed-wave WindCube V2. Both these instruments make use of specific probe volumes to determine wind speeds at certain locations. The WindCube is a vertical profiling lidar and therefore needs large conical averaging volumes to determine accurate mean wind speeds. The SpinnerLidar has better specifics for taking accurate individual measurements, but still needs large volume averaging of wind direction to transform the measurements to true wind speeds. Combining both these different probing volumes in a comparison might explain the offset of about -0.2 m/s as shown in Chapter 6 and Appendix D in the wind speed comparison at hub height, as well as the offset of about -0.5 m/s in the wind profiles of the different wind speed classes as shown in Chapter 7 and Appendix E. However, a counter argument for this being a result of probing volume inaccuracy is the fact that the offset is constant over all periods, heights and wind conditions. Wrongful calibration could be a reason for a continuous offset, but as will follow in section 8.4, there can also be a physical explanation.

8.2 Free inflow

As discussed excessively in Chapter 5 a method had to be developed to convert the raw LoS measurements from the SpinnerLidar to true wind speed values. In this research is was chosen to use a simplified approach based on basic knowledge about free inflow wind conditions.

8.2.1 Limited data use

Surrounding wind turbines and obstacles at the EWTW are causing wake effects and disturbances in the inflow field of Turbine R9 in major periods during the measurement campaign. The proposed method had to determine the horizontal stream direction of the wind by fitting a curve to the measured incoming LoS measurements. Wake effects will disturb this curve fitting, which makes it difficult to properly assess the averaged horizontal stream direction. Therefore with this approach, only the periods of free inflow could be used for characterization. For the purpose of this research, this was sufficient, but of course the disregarded data also holds valuable information.
Other methods of converting LoS measurements might be able to better convert the periods of disturbed inflow. But even with these methods converting disturbed flow will have it's implications.

8.2.2 Free inflow assumptions

The assumptions which were made about the standard conditions of free flowing wind can be considered a bit too simplified. All measurements were projected on one averaged horizontal stream direction to assess their true magnitude instead of the LoS component measurement. But in a truly representative wind field reconstruction, not all direction vectors will be in the exact same direction. Turbulent structures can cause very local deviations in the wind direction, which by this approach are filtered out and projected to a wrong average direction.
The only possible way to address a true wind direction vector for every measurement is using an instrument which measures from different locations at the same time to obtain a full 3 component wind speed measurement.

8.3 Wind veering

With the applied method to convert the raw LoS measurements to true wind speed vectors, an average horizontal stream direction is used over the whole vertical range of the measurement plane. However, as can be seen in Figure 5.2, the vertical range of the SpinnerLidar measurements reaches from 60 to 130 meters. On such a range it is known that Ekman spiraling of the wind direction can and most likely will be present, meaning that applying one wind horizontal wind direction for all measurements is not entirely correct.

The averaged horizontal stream direction was determined by making use of the data between 70 and 95 meters (due to data gaps in the lower regions). This makes the corrected wind speed measurements between this range relatively accurate. But below and above this range, the same horizontal stream direction is used but might not be representative for these regions of the vertical wind profile. This is very likely to be an explanation for the fact that the vertical profiles measured by the SpinnerLidar as shown in Figure 7.3 and in the figures of Appendix E show a deviation in the upper part of the vertical profiles with respect to the WindCube.

The WindCube determines the averaged horizontal stream direction separately at every 10 meter height level and uses this direction to quantify the wind speed measurements. A a test for this hypothesis the wind veering as measured by the WindCube can be fed to the SpinnerLidar data in order to make better projections at every separate height level in the measurement plane. The results are promising as can be seen in Figure 8.1, where the SpinnerLidar vertical profile is closer to the WindCube vertical profile for the wind veer corrected measurements in the lower and upper regions. However, preferably a method has to be developed to determine the wind veering from the SpinnerLidar data alone instead of using a second instrument. This could be accomplished by dividing the measurement plane in different height bands and thus being able to determine a wind direction for each height band separately.

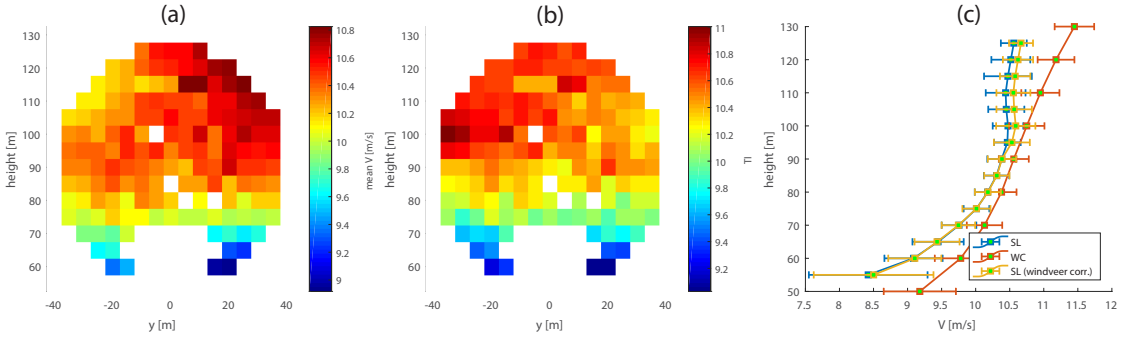

Figure 8.1: Feeding wind veer data of WindCube to SpinnerLidar transformation algorithm, (a) shows the transformed wind speeds as by the method proposed in Chapter 5, note the increasing wind speeds in the upright corner, (b) shows the transformed wind speeds if three different wind direction angles are used over the plane, (c) shows the difference in wind profiles when using wind veer knowledge, note the increased accuracy in the upper part of the profile when taking wind veer into account

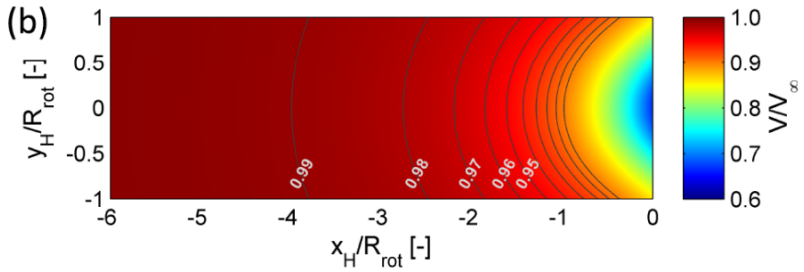

Figure 8.2: Analytical flow field in the induction zone of a wind turbine at hub height (Borraccino et al. [2017])

8.4 Blockage effect of a rotating turbine

As briefly touched upon above, there is a remarkable difference in the wind speeds measured by the SpinnerLidar and the WindCube, as indicated by the -0.2 m/s difference in the validation studies and -0.5 m/s in the vertical profile comparison. Instrumental errors could of course be a very logical explanation for this observation. But there is one other phenomenon which could explain why the wind speeds of the corrected SpinnerLidar measurements are slightly lower than those of the WindCube.

Considering the measurement location of the two instruments it has to be noted that the WindCube is always measuring a vertical profile at around 200 meters East of the location of turbine R9. The measurement location of the SpinnerLidar changes with the yawing of the turbine, but is always approximately 60 meters in front of the turbine.

By harnessing energy from the wind, an operating turbine creates an induction zone upstream of its rotor (Sørensen [2016]). Closer to the turbine, wind speeds will get lower due to the blockage effect of the rotating blades. The extent to which this effect reaches upstream is dependent on the rotor diameter, but can be measured to lengths of 2 times the rotor diameter in the upstream direction. The Nordex turbines have a rotor diameter of 80 meters. With the SpinnerLidar measuring at around 60 meters in front of the turbine this would mean that the measurement location is always at 0.8 D_{rot} or 1.6 R_{rot}. Borraccino et al. [2017] use a simplified induction model in their research which shows that at 1.5 R_{rot} the effect of induction on the inflow wind can be 0.95, see Figure 8.2. At averaged wind speeds of 10 m/s this would mean that the induction zone can cause a reduction of wind speed by 5%, meaning 0.5 m/s. The WindCube, which with 2.5 D_{rot} is always out of reach for the induction zone, might therefore measure higher wind speeds than the SpinnerLidar.

An extra confirmation of this blockage effect could lie in the fact that the linear relation in the comparison between the SpinnerLidar and the WindCube wind speed measurements as shown in Appendix D is slightly below 1 (around 0.97). This linear relation being below 1 means that in the higher ranges of these comparisons the wind speed measurements are showing a larger offset than in the lower ranges of these comparisons. This matches with the induction model which shows the blockage effect to be a percentage of the wind speed, so with higher wind speeds the absolute offset becomes larger.

8.5 Turbulence intensity against noise

Lidar wind measurements are to a certain amount always prone to noise (Sathe et al. [2015]). The combination of sensors together with the varying backscattered components are never exactly constant. This noise can propagate into the fluctuations of the wind speed measurements.

The turbulence intensity is dependent on standard deviations of the wind, which is based on the fluctuations of individual measurements in respect to the mean value. If the noise of an instrument is increasing the fluctuations of the measurements it can therefore influence the amount of turbulence intensity. Because the noise levels of both lidar instruments are not well known, it's not very certain which percentage of the fluctuations in the measurements is caused by noise and which is caused by real turbulent fluctuations. Careful calibration studies are needed to distuinguish noise from turbulent intensity.

CHAPTER 9

Conclusion

The SpinnerLidar is a forward looking wind lidar instrument capable of obtaining tons of information about the inflow wind field of wind turbines. However, as it is still in development, the raw line-of-sight data needs processing before valid information about the wind can be reviewed. Therefore a first objective of this research was stated as:

How can 3D wind vectors be constructed from SpinnerLidar data?

Tackling this 'Cyclops syndrome' was done by the use of a simplified approach based on the assumptions that during free inflow conditions the wind will be (almost) completely stratified and taking into account a possible yaw misalignment. This allowed the LoS measurements to be projected on a general wind direction revealing their true magnitude. With these true 3D wind vectors being obtained the next was to validate them against other wind measuring instruments:

How can the SpinnerLidar measurements be (cross-)validated?

The converted measurements could be compared against simultaneously taken measurement of a nearby vertical profiling WindCube V2. A regression analysis indicated an installation offset of about 5 degrees of the SpinnerLidar but this did not influence the high correlation found between the two instruments. A constant offset of about 0.2 m/s in wind speed measurements between the SpinnerLidar and WindCube was found, which could be explained as being a result of the blockage effect of wind turbine. Unless this constant offset, the trend of both instruments was very alike. This meant that the proposed method for correcting the LoS measurements was validated and thereby the obtained data of free inflow wind could be used for the last objective of this research:

What are the spatio-temporal turbulent characteristics of the turbine inflow wind fields?

To characterize the inflow wind field for the free inflow periods the measurements were divided into grid boxes to be able to visualize the mean wind field and to calculate the deviations in turbulence intensity over the measurement plane. It was found that lower regions of the measurement plane of the SpinnerLidar contained higher turbulence, comparison with the WindCube showed the same results, this is most likely due to surface friction. Also it is likely that the blockage effect of the rotating blades is visible in the mean wind speed data by a 0.5 m/s difference when comparing the SpinnerLidar measurements with the WindCube measurements. A difference in day and night turbulence was not found, most likely due to the winter conditions during the measurement campaign.

Overall it can be concluded that the SpinnerLidar holds the potential to very abundantly measure the inflow wind field. This research touched upon a part of its potential and can therefore be seen as a

pioneering study. The ‘Cyclops syndrome’ still causes need for large averaging of the data and further research will be needed to tackle this syndrome to be able to capture the full potential of this instrument.

CHAPTER 10

Recommendations

Measuring the inflow wind field with a state-of-the-art instrument like the SpinnerLidar is still in development. For future research the following recommendations are suggested.

When installing the SpinnerLidar close attention should be paid to knowing the exact direction and orientation of the instrument. The internal coordinate system on which the SpinnerLidar is based is not common in the wind lidar industry, because it is a rotated coordinate system from an upward looking device. Advantage could be achieved when giving the SpinnerLidar an automated conversion tool for deriving the exact location of the measurements locations. Because exact locations will be necessary to make good estimates of the accuracy and precision of the SpinnerLidar as a wind measuring instrument.

The accuracy of the SpinnerLidar instrument is also not well known yet. Even though it uses a known ZephIR lidar instrument, the application differs, making the older calibration studies not suited for the SpinnerLidar. A validation of this SpinnerLidar instrument inside a wind tunnel could therefore be very useful. Or setting up the SpinnerLidar to measure at the exact same location as a validated meteo mast would suffice as well. Certainly because turbulence intensity can be dependent on the noise of the measurement instrument more knowledge about this is needed.

Tackling the Cyclops syndrome will always remain an issue for the SpinnerLidar when used as a stand-alone device. But the best way to address this might be using multiple focusing distances in a simultaneous measuring approach. This is of course dependent on the ability of the instrument to change focus at a quick rate. But with the current sampling rate of 400 Hz this will not be a big problem.

The rose curve is a clever way to scan a big plane in just a fraction of a second by using only two prisms. But it makes it hard to search for turbulent structures in the measurements of a 'frozen' second. Ideally, a more spatially constant grid with a slightly higher density would be used, which would allow for very interesting energy spectra to be conducted from the measurements.

At last wind veering is an atmospheric phenomena which has to be addressed in future studies of the SpinnerLidar data. All current studies do not account for this phenomena while it can have a large impact on transforming the Line-of-Sight measurements. See Chapter 8 for a proposed method.

Bibliography

N. Angelou and M. Sjöholm. Unitte wp3/mc1: Measuring the inflow towards a nordtank 500kw turbine using three short-range windscanners and one spinnerlidar. *DTU Wind Energy*, 0093, 2015.

N. Angelou, T. Mikkelsen, K. H. Hansen, M. Sjöholm, and M. Harris. Lidar wind speed measurements from a rotating spinner (spinnerex 2009). *Kgs. Lyngby, Denmark: Technical University of Denmark*, 2010.

L. Arturo Soriano, W. Yu, and J. d. J. Rubio. Modeling and control of wind turbine. *Mathematical Problems in Engineering*, 2013, 2013.

A. Borraccino, D. Schlipf, F. Haizmann, and R. Wagner. Wind field reconstruction from nacelle-mounted lidar short-range measurements. *Wind Energy Science*, 2(1):269, 2017.

E. Bot. *Turbulence assessment with ground based LiDARs*. ECN, 2014.

S. Emeis. Isars 13 special issues. *Meteorologische Zeitschrift*, 16(4):323–324, 2007.

R. Floors, A. Peña, G. Lea, N. Vasiljević, E. Simon, and M. Courtney. The rune experimenta database of remote-sensing observations of near-shore winds. *Remote Sensing*, 8(11):884, 2016.

P. G. Hofmeister, C. Bollig, S. Fayed, M. Kunze, and R. Reuter. A compact doppler wind lidar for controlling the operation of wind turbines. *EARSeL eProceedings*, 14(1):1, 2015.

S. Kapp and M. Kühn. A five-parameter wind field estimation method based on spherical upwind lidar measurements. In *Journal of Physics: Conference Series*, volume 555, page 012112. IOP Publishing, 2014.

T. Mikkelsen, N. Angelou, K. Hansen, M. Sjöholm, M. Harris, C. Slinger, P. Hadley, R. Scullion, G. Ellis, and G. Vives. A spinner-integrated wind lidar for enhanced wind turbine control. *Wind Energy*, 16 (4):625–643, 2013.

T. Mikkelsen, P. Astrup, and M. F. van Dooren. The lidar cyclops syndrome bypassed: 3d wind field measurements from a turbine mounted lidar in combination with a fast cfd solver. In *ISARS 2016: 18. international symposium for the advancement of boundary layer remote sensing, Varna June 2016*, volume 1, 2016.

A. Sathe, J. Mann, T. Barlas, W. Bierbooms, and G. Bussel. Influence of atmospheric stability on wind turbine loads. *Wind Energy*, 16(7):1013–1032, 2013.

A. Sathe, R. Banta, L. Pauscher, K. Vogstad, D. Schlipf, and S. Wylie. Estimating turbulence statistics and parameters from ground-and nacelle-based lidar measurements: Iea wind expert report. 2015.

D. Schlipf, S. Kapp, J. Anger, O. Bischoff, M. Hofsäß, A. Rettenmeier, and M. Kühn. Prospects of optimization of energy production by lidar assisted control of wind turbines. 2011.

E. Simley, H. Frst, F. Haizmann, and D. Schlipf. Optimizing lidars for wind turbine control applicationsresults from the iea wind task 32 workshop. 10:863, 06 2018.

J. N. Sørensen. *General momentum theory for horizontal axis wind turbines*, volume 4. Springer, 2016.

J. Wagenaar. Infrastructure project: Irpwind scanflow. 2017.

J. M. Wallace and P. V. Hobbs. *Atmospheric science: an introductory survey*, volume 92. Elsevier, 2006.

E. Werkhoven, J. Wagenaar, and M. van Roermond. Scanflow measuring plan. 2017.

APPENDIX A

SpinnerLidar data file

An example of a data file of the SpinnerLidar as available from the ScanFlow project. All variables (Azimuth, Focus, Inclination, Power, Quality, Sx, Sy and VLOS), as described in section 4.3, are found in the second row. Below that all individual measurements are allocated with a timestap in the first column.

				SCNFLW							
TimestampUTC	**Spin_Azim...**	**Spin_Foc...**	**Spin_Incl...**	**Spin_Power**	**Spin_Qual...**	**Spin_Sam...**	**Spin_Scal...**	**Spin_Sx**	**Spin_Sy**	**Spin_T...**	**Spin_VLOS**
Text	Number	Number	Number	Number	Number	Number	Number	Number	Number	Number	Number
scanflow^4.4.0@betelgeus...	488.3	488.3	488.3	488.3	488.3	488.3	488.3	488.3	488.3	488.3	488.3
Timestamp(UTC)	Spin_Azi...	Spin_Fo...	Spin_Inc...	Spin_Power	Spin_Qua...	Spin_Sam...	Spin_Sca...	Spin_Sx	Spin_Sy	Spin_T...	Spin_VLOS
t	deg	m	deg	-	-	-	-	-	-	m	m/s
2017-02-01 20:10:00.0000000	5.41822	71.55500	0.10526	48.49340	0.32070	305.00000	0.00010	-0.01780	0.35883	8.11211	9.33800
2017-02-01 20:10:00.0020480	5.41496	71.55500	0.10511	85.83240	0.25314	306.00000	0.00025	-0.06607	0.36647	8.11211	2.27323
2017-02-01 20:10:00.0040960	5.41154	71.55500	0.10497	914.82300	0.57344	307.00000	0.00340	-0.11622	0.36689	8.11211	2.07828
2017-02-01 20:10:00.0061440	5.40883	71.55500	0.10468	1258.00000	0.57035	308.00000	0.00474	-0.16733	0.35976	8.11211	2.06463
2017-02-01 20:10:00.0081920	5.40626	71.55500	0.10447	1441.70996	0.61286	309.00000	0.00535	-0.21797	0.34495	8.11211	2.01165
2017-02-01 20:10:00.0102400	5.40384	71.55500	0.10499	1515.59998	0.56549	310.00000	0.00541	-0.26715	0.32241	8.11211	1.92449
2017-02-01 20:10:00.0122880	5.40180	71.55500	0.10599	1491.16003	0.54841	311.00000	0.00519	-0.31343	0.29251	8.11211	1.76525
2017-02-01 20:10:00.0143360	5.40021	71.55500	0.10684	1394.29004	0.56607	312.00000	0.00493	-0.35589	0.25551	8.11211	1.58322
2017-02-01 20:10:00.0163840	5.39887	71.55500	0.10796	1272.90002	0.52416	313.00000	0.00412	-0.39322	0.21221	8.11211	1.35508
2017-02-01 20:10:00.0184320	5.39783	71.55500	0.10963	66.76130	0.37601	314.00000	0.00018	-0.42463	0.16317	8.11211	1.23024
2017-02-01 20:10:00.0204800	5.39700	71.55500	0.11147	23.10680	0.32563	315.00000	0.00018	-0.44913	0.10954	8.11211	0.73743
2017-02-01 20:10:00.0225280	5.39657	71.55500	0.11302	43.96180	0.43292	316.00000	0.00038	-0.46613	0.05213	8.11211	0.70775
2017-02-01 20:10:00.0245761	5.39668	71.55500	0.11455	42.06080	0.42625	317.00000	0.00034	-0.47503	-0.00766	8.11211	0.71430
2017-02-01 20:10:00.0266241	5.39700	71.55500	0.11707	47.20330	0.42593	318.00000	0.00040	-0.47552	-0.06887	8.11211	0.70852
2017-02-01 20:10:00.0286721	5.39749	71.55500	0.11953	52.47000	0.47168	319.00000	0.00046	-0.46744	-0.12997	8.11211	0.70192
2017-02-01 20:10:00.0307201	5.39825	71.55500	0.12137	54.51330	0.45749	320.00000	0.00047	-0.45081	-0.18996	8.11211	0.70563
2017-02-01 20:10:00.0327681	5.39924	71.55500	0.12286	32.61300	0.54965	321.00000	0.00021	-0.42593	-0.24731	8.11211	0.82168
2017-02-01 20:10:00.0348161	5.40056	71.55500	0.12462	46.92560	0.19923	322.00000	0.00007	-0.39312	-0.30108	8.11211	7.06412
2017-02-01 20:10:00.0368641	5.40226	71.55500	0.12707	62.32650	0.04872	323.00000	0.00010	-0.35313	-0.34989	8.11211	6.41827

APPENDIX B

WindCube data file

An example of a data file of the WindCube as available from the ScanFlow project. All variables (Data_Avail, Wd, Ws, WsDisp, ZWs, ZWsDisp), as described in section 4.4, are found in the second row. In the same variable names 'H100' indicates a height level of 100 meters for which these variables are determined. At the far right one can see that the next height at 110 meters will be addressed.

							cube								
TimestampUTC	...	...	...	WC258H100_Data_Avail	...	WC258H100_Wd	WC258H100_Ws	...	...	WC258H100_WsDisp	WC258H100_ZWs	WC258H100_ZWsDisp	...	...	WC258H110
Text				Number		Number	Number			Number	Number	Number			Number
scanflow^4.4.0@betel...	...	...	...	0.001667	...	0.001667	0.001667	...	...	0.001667	0.001667	0.001667	...	...	0.001667
Timestamp(UTC)	...	...	...	WC258-H100_Data_Avail	...	WC258-H100_Wd	WC258-H100_Ws	...	...	WC258-H100_WsDisp	WC258-H100_Z-Ws	WC258-H100_Z-WsDisp	...	...	WC258-H110
t	...	...	...	%	...	deg	m/s	...	...	m/s	m/s	m/s	...	...	%
2016-12-01 00:00:00.00	...	...	...	100.00000	...	278.10001	7.85000	...	...	0.75000	0.04000	0.38000	...	...	100.00000
2016-12-01 00:10:00.00	...	...	...	100.00000	...	280.39999	8.70000	...	...	0.87000	0.19000	0.43000	...	...	100.00000
2016-12-01 00:20:00.00	...	...	...	100.00000	...	278.00000	8.63000	...	...	0.92000	0.15000	0.42000	...	...	100.00000
2016-12-01 00:30:00.00	...	...	...	100.00000	...	279.60001	8.73000	...	...	0.55000	0.11000	0.28000	...	...	100.00000
2016-12-01 00:40:00.00	...	...	...	100.00000	...	279.20001	8.52000	...	...	0.90000	0.13000	0.44000	...	...	100.00000
2016-12-01 00:50:00.00	...	...	...	100.00000	...	277.60001	8.75000	...	...	0.91000	0.16000	0.39000	...	...	100.00000
2016-12-01 01:00:00.00	...	...	...	100.00000	...	279.39999	8.62000	...	...	0.60000	0.08000	0.29000	...	...	100.00000
2016-12-01 01:10:00.00	...	...	...	100.00000	...	279.60001	8.02000	...	...	0.72000	0.09000	0.28000	...	...	100.00000
2016-12-01 01:20:00.00	...	...	...	100.00000	...	281.10001	7.06000	...	...	0.70000	0.16000	0.39000	...	...	100.00000
2016-12-01 01:30:00.00	...	...	...	100.00000	...	281.29999	7.41000	...	...	0.47000	0.09000	0.24000	...	...	100.00000
2016-12-01 01:40:00.00	...	...	...	100.00000	...	280.39999	6.87000	...	...	0.58000	0.10000	0.28000	...	...	100.00000
2016-12-01 01:50:00.00	...	...	...	100.00000	...	276.20001	6.89000	...	...	1.61000	0.18000	0.67000	...	...	100.00000
2016-12-01 02:00:00.00	...	...	...	100.00000	...	278.60001	8.39000	...	...	1.05000	0.24000	0.53000	...	...	100.00000
2016-12-01 02:10:00.00	...	...	...	100.00000	...	278.70001	8.34000	...	...	0.78000	0.21000	0.33000	...	...	100.00000
2016-12-01 02:20:00.00	...	...	...	100.00000	...	279.50000	8.85000	...	...	0.51000	0.01000	0.29000	...	...	100.00000
2016-12-01 02:30:00.00	...	...	...	100.00000	...	281.60001	8.54000	...	...	0.58000	0.12000	0.28000	...	...	100.00000
2016-12-01 02:40:00.00	...	...	...	100.00000	...	282.39999	8.22000	...	...	0.47000	0.01000	0.27000	...	...	100.00000
2016-12-01 02:50:00.00	...	...	...	100.00000	...	283.39999	8.35000	...	...	0.49000	0.08000	0.26000	...	...	100.00000
2016-12-01 03:00:00.00	...	...	...	100.00000	...	283.29999	8.18000	...	...	0.42000	0.09000	0.23000	...	...	100.00000
2016-12-01 03:10:00.00	...	...	...	100.00000	...	283.39999	7.95000	...	...	0.43000	0.08000	0.25000	...	...	100.00000
2016-12-01 03:20:00.00	...	...	...	100.00000	...	283.70001	8.12000	...	...	0.45000	0.11000	0.22000	...	...	100.00000
2016-12-01 03:30:00.00	...	...	...	100.00000	...	283.29999	7.73000	...	...	0.48000	0.10000	0.22000	...	...	100.00000
2016-12-01 03:40:00.00	...	...	...	100.00000	...	281.10001	7.64000	...	...	0.45000	0.12000	0.20000	...	...	100.00000
2016-12-01 03:50:00.00	...	...	...	100.00000	...	282.89999	7.77000	...	...	0.47000	0.09000	0.24000	...	...	100.00000
2016-12-01 04:00:00.00	...	...	...	100.00000	...	281.39999	8.07000	...	...	0.43000	0.11000	0.21000	...	...	100.00000
2016-12-01 04:10:00.00	...	...	...	100.00000	...	279.29999	8.00000	...	...	0.36000	0.15000	0.21000	...	...	100.00000
2016-12-01 04:20:00.00	...	...	...	100.00000	...	281.29999	7.68000	...	...	0.47000	0.10000	0.22000	...	...	100.00000

APPENDIX C

The chirality of the SpinnerLidar coordinate system

The following page contains a document written by Mikael Sjöholm for the Danish Technical University. The document explains the set-up of the SpinnerLidar internal coordinate system.

The chirality of the SpinnerLidar coordinate system

The SpinnerLidars provide relative normalized coordinates S_x, S_y, S_z of a unit vector $\vec{s}$ pointing from the scannerhead towards the measurement location that multiplied by the focus distance R gives the vector towards the measurement location. For reducing unnecessary data, S_z is not stored but can be calculated from the relation $S_x^2 + S_y^2 + S_z^2 = 1$.

The S_x, S_y coordinates are calculated from the azimuth angles of the prisms which are obtained by running the motor at constant speed and by using a counter for each prism that are reset once per revolution by the signal from a proximity sensor on each prism. One of the prisms makes 13 revolutions and the other prism makes 7 revolutions for a complete scanning pattern which starts when both prisms are in the zero angle position simultaneously.

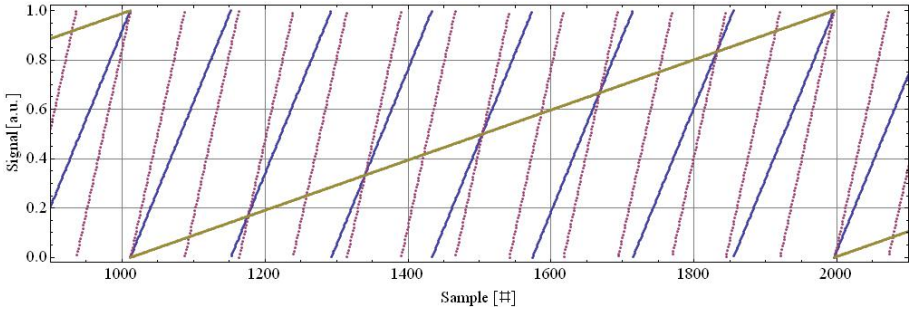

Figure 1. The prism counters resets 13 and 7 times respectively for a complete scanning rosette pattern.

The angle proximity sensors are located such that the x-axis is towards the side of the SpinnerLidar where the motor is located and the z-axis is along the symmetry axis of the SpinnerLidar towards the measurement location. The direction of the y-axis is determined, due to the angle measurement procedure, by the rotation direction of the motor as illustrated in figure 2. If the motor is running in the positive direction the coordinate system becomes left-handed and if the motor is running in the negative direction the coordinate system becomes right-handed.

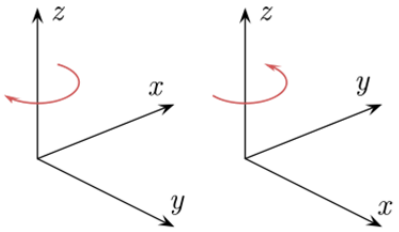

Figure 2. If the motor is running in the positive direction the coordinate system becomes left-handed (left figure) and if the motor is running in the negative direction the coordinate system becomes right-handed (right figure)

When the SpinnerLidar was operated directly from the Kollmorgen drive it was run in positive direction creating a left-handed coordinate system but when operated with the new Labview interface the positive rpm input value is negated inside the software in order to run the motor in the negative direction with the purpose of creating a right-handed coordinate system. The SpinnerLidar motor was operated directly from the Kollmorgen drive before the Labview interface was developed for the second SpinnerLidar at the end of 2015. However the first SpinnerLidar was not upgraded with the new interface until after the end of the Colorado campaign in 2016.

Version 1.0 Written by Mikael Sjöholm (misj@dtu.dk)

APPENDIX D

Regression Analysis of SpinnerLidar en WindCube wind speed measurements

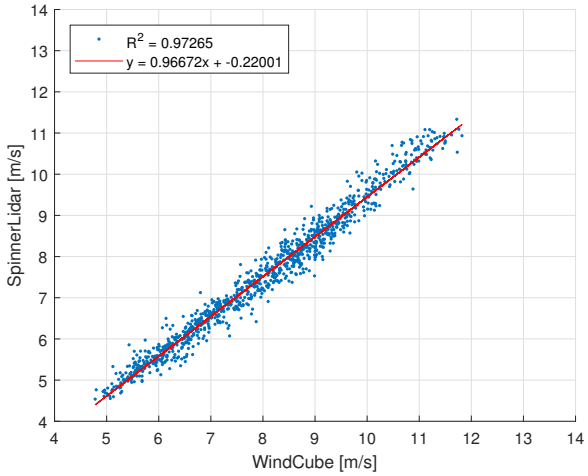

Figure D.1: Comparison of wind speeds measured at a height level of 60 meters

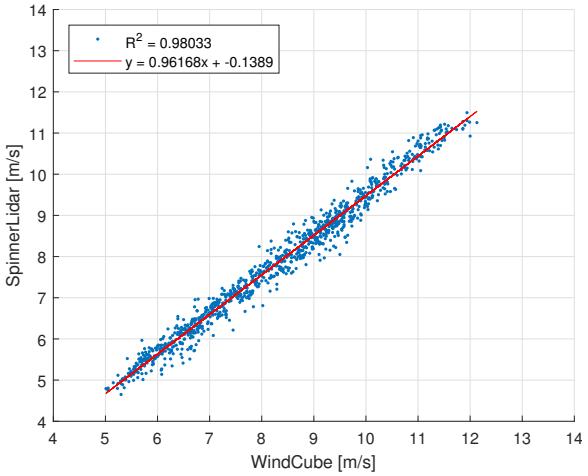

Figure D.2: Comparison of wind speeds measured at a height level of 70 meters

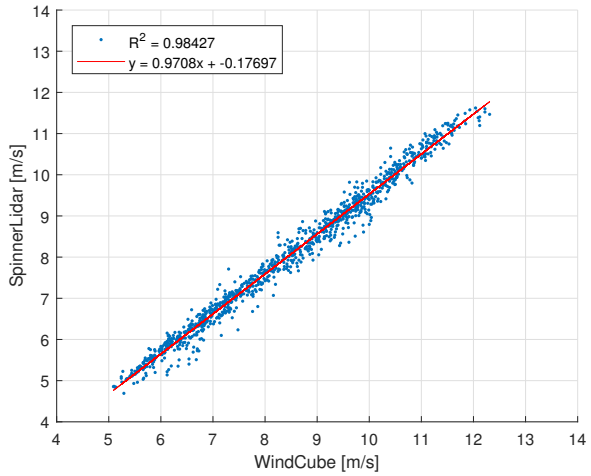

Figure D.3: Comparison of wind speeds measured at a height level of 80 meters

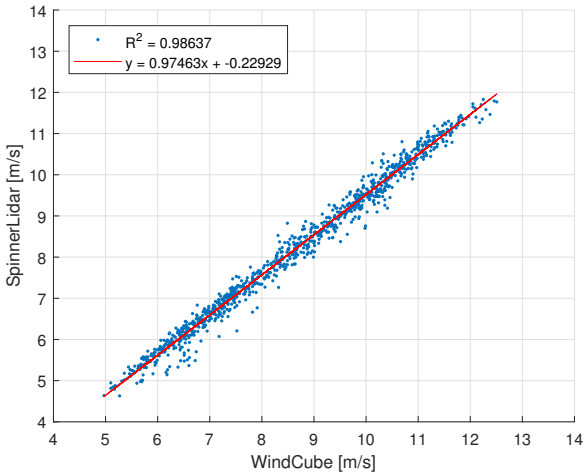

Figure D.4: Comparison of wind speeds measured at a height level of 90 meters

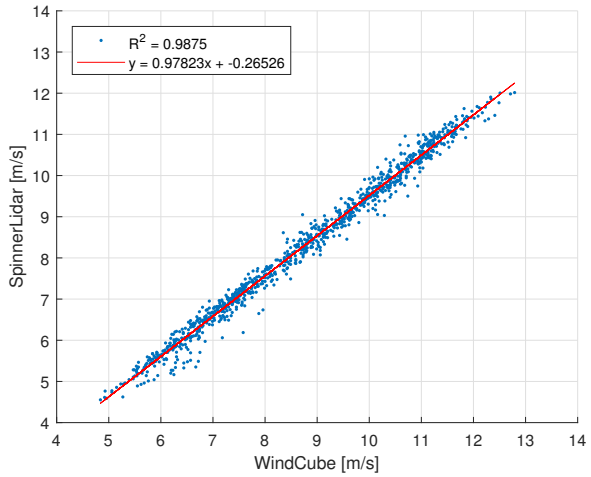

Figure D.5: Comparison of wind speeds measured at a height level of 100 meters

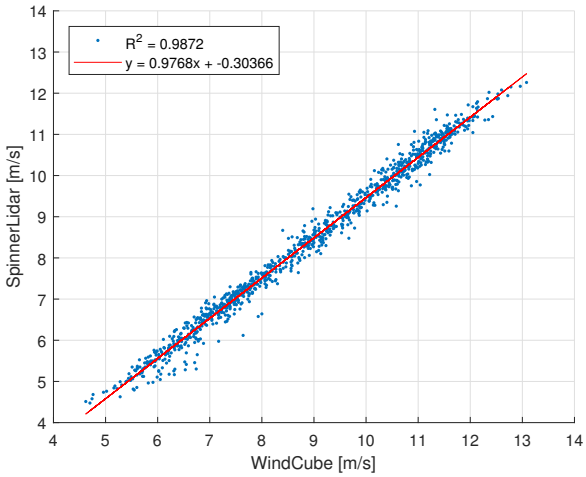

Figure D.6: Comparison of wind speeds measured at a height level of 110 meters

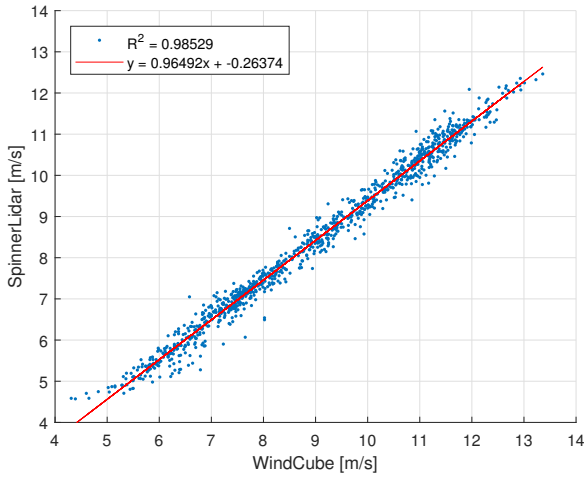

Figure D.7: Comparison of wind speeds measured at a height level of 120 meters

APPENDIX E

Wind speed classification

In the following figures (a) shows the mean wind speed of this class at every 5 by 5 meter grid box over the whole measurement plane, (b) shows the average wind speed profile of this class for the SpinnerLidar as well as the WindCube, the error-bars indicate the standard deviation calculated from all available measurements for this class, (c) shows the turbulent intensity calculated for each 5 by 5 meter grid box, (d) shows the turbulent intensity profiles of this class for the SpinnerLidar as well as the WindCube

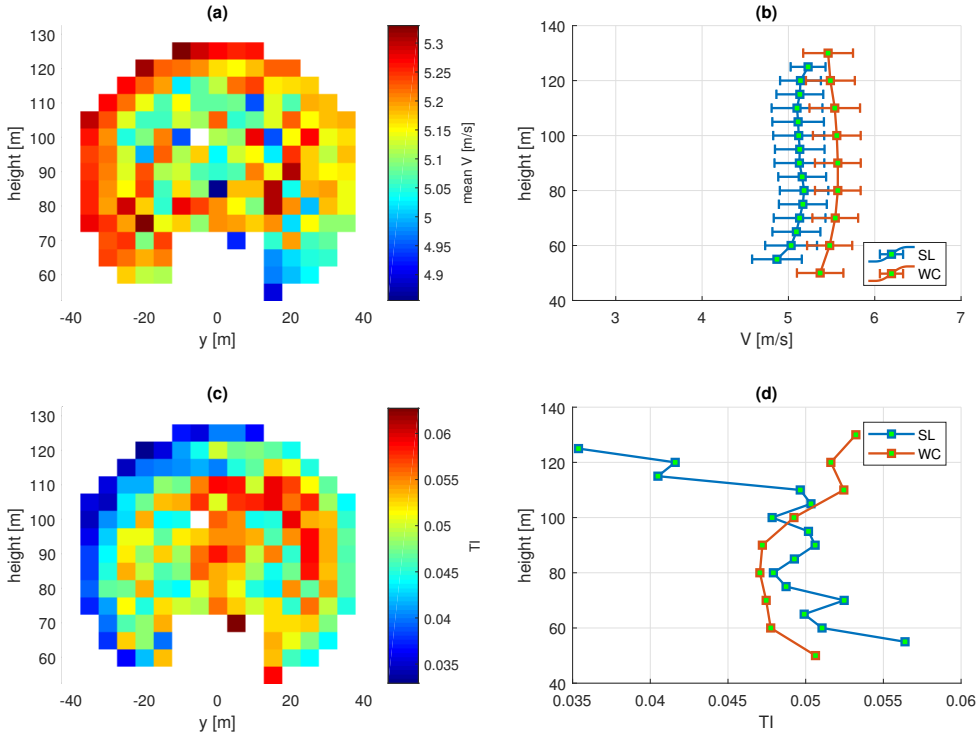

Figure E.1: Characterization of wind speed class of averaged wind speeds of 5 m/s, in total 34 periods were found for this class (see top of this Appendix for explanation on the different figures)

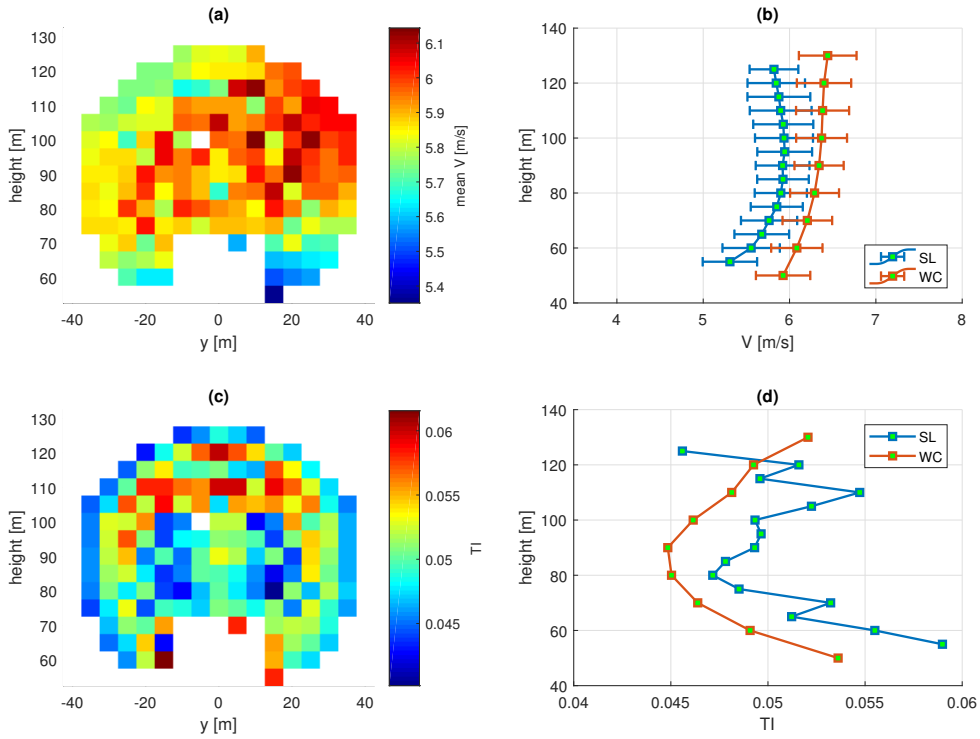

Figure E.2: Characterization of wind speed class of averaged wind speeds of 6 m/s, in total 64 periods were found for this class (see top of this Appendix for explanation on the different figures)

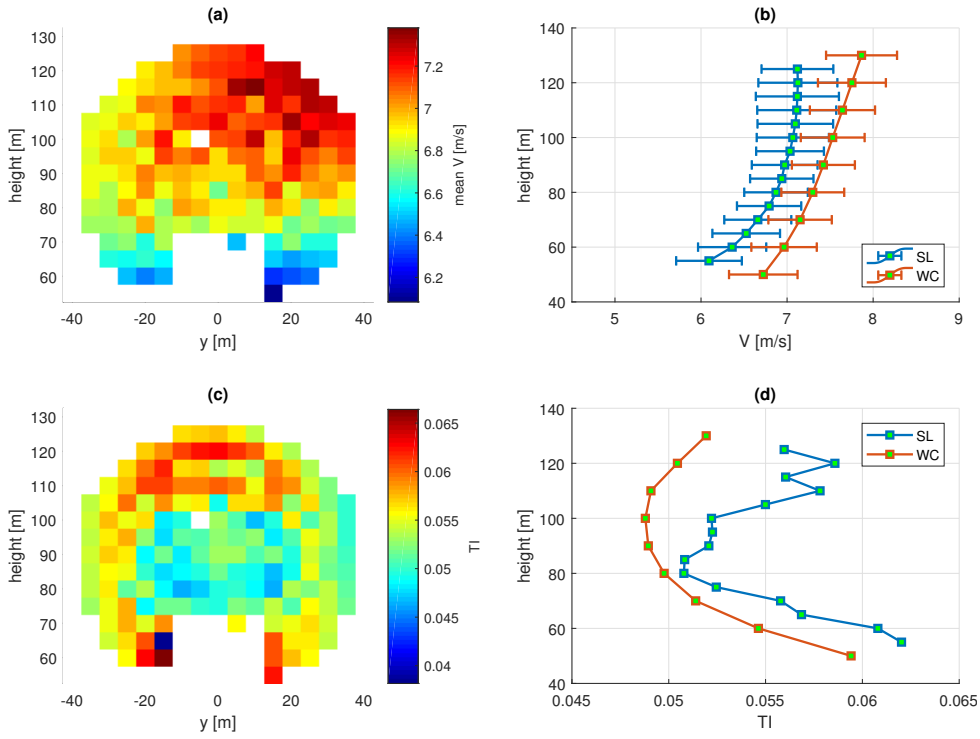

Figure E.3: Characterization of wind speed class of averaged wind speeds of 7 m/s, in total 42 periods were found for this class (see top of this Appendix for explanation on the different figures)

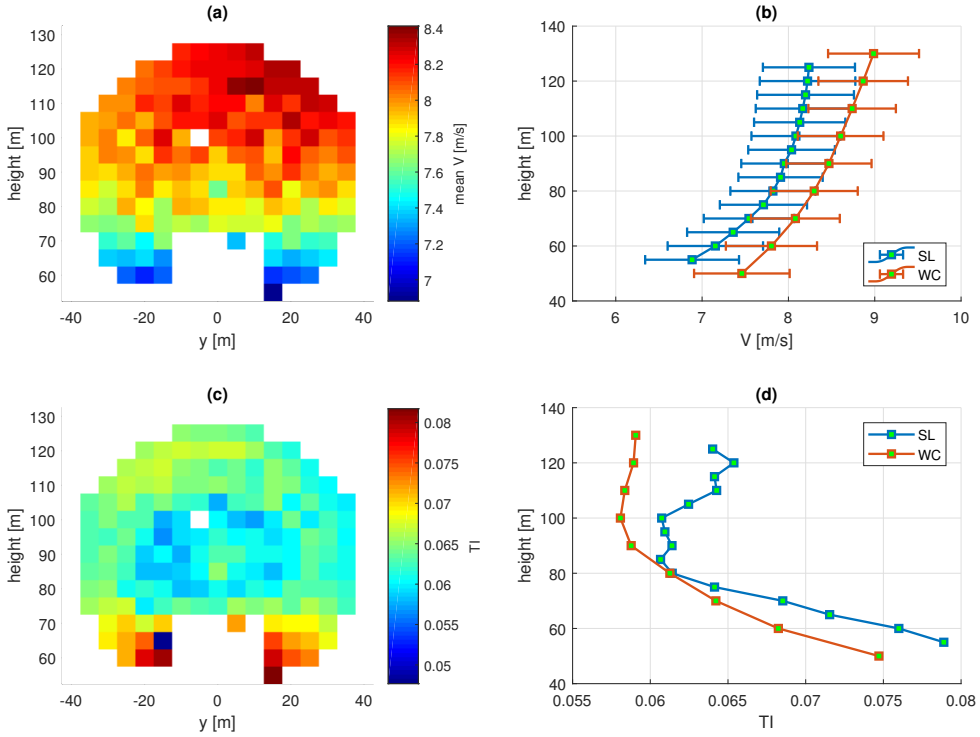

Figure E.4: Characterization of wind speed class of averaged wind speeds of 8 m/s, in total 32 periods were found for this class (see top of this Appendix for explanation on the different figures)

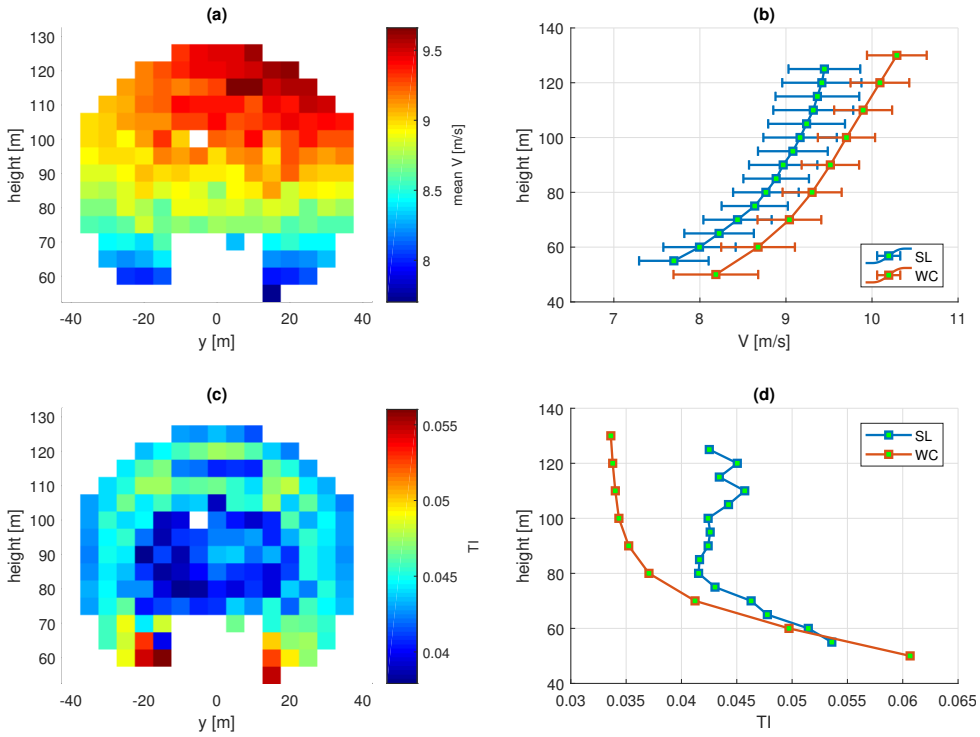

Figure E.5: Characterization of wind speed class of averaged wind speeds of 9 m/s, in total 117 periods were found for this class (see top of this Appendix for explanation on the different figures)

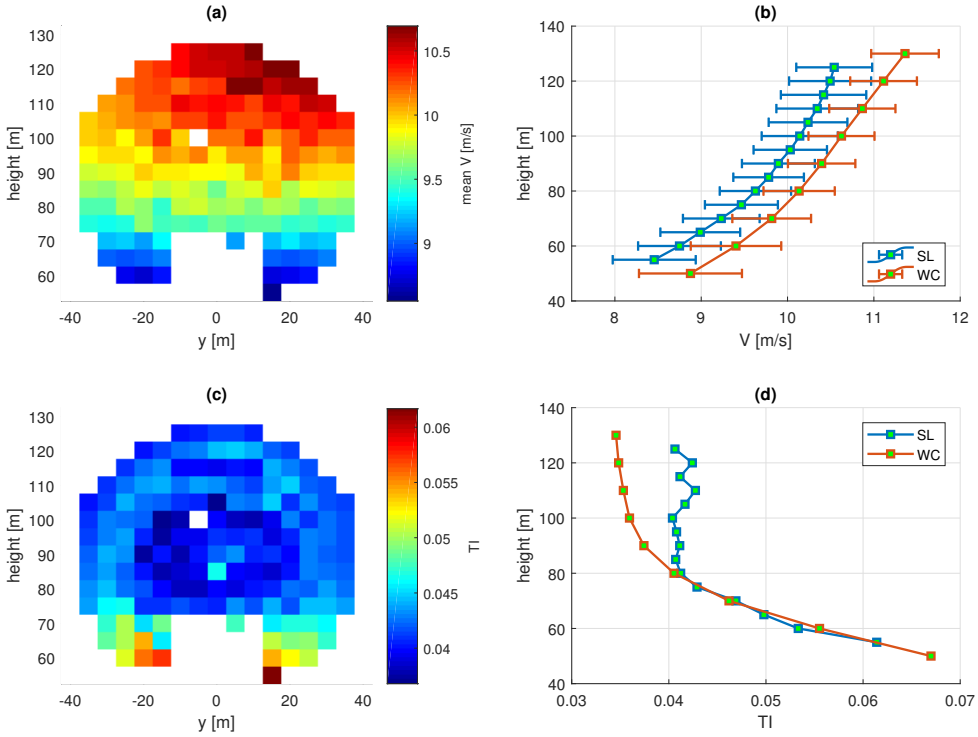

Figure E.6: Characterization of wind speed class of averaged wind speeds of 10 m/s, in total 177 periods were found for this class (see top of this Appendix for explanation on the different figures)

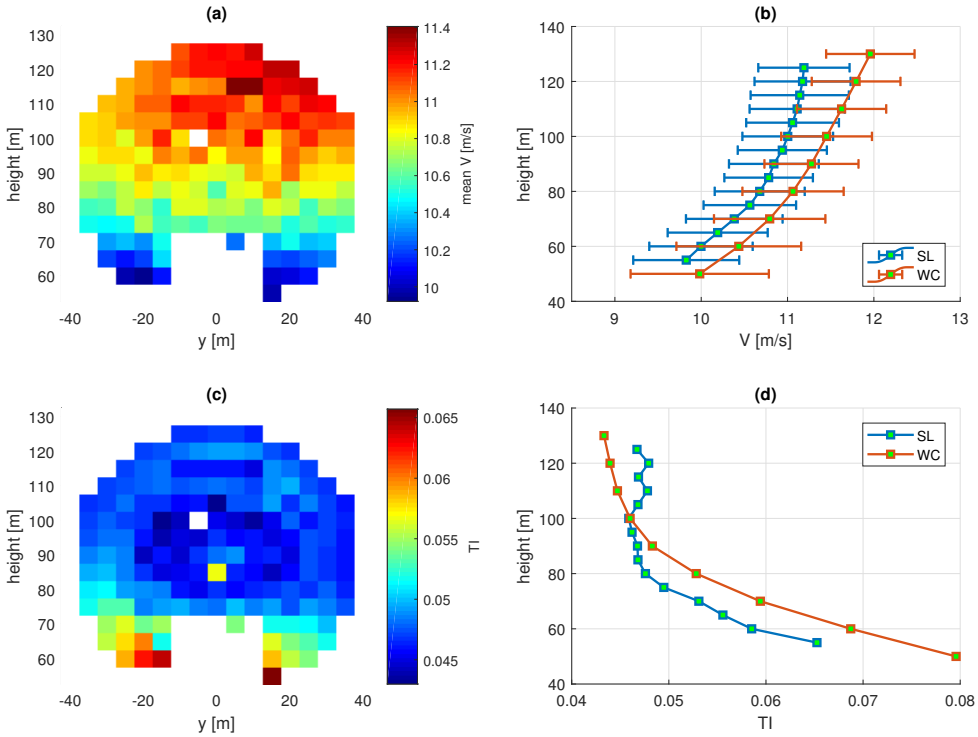

Figure E.7: Characterization of wind speed class of averaged wind speeds of 11 m/s, in total 113 periods were found for this class (see top of this Appendix for explanation on the different figures)

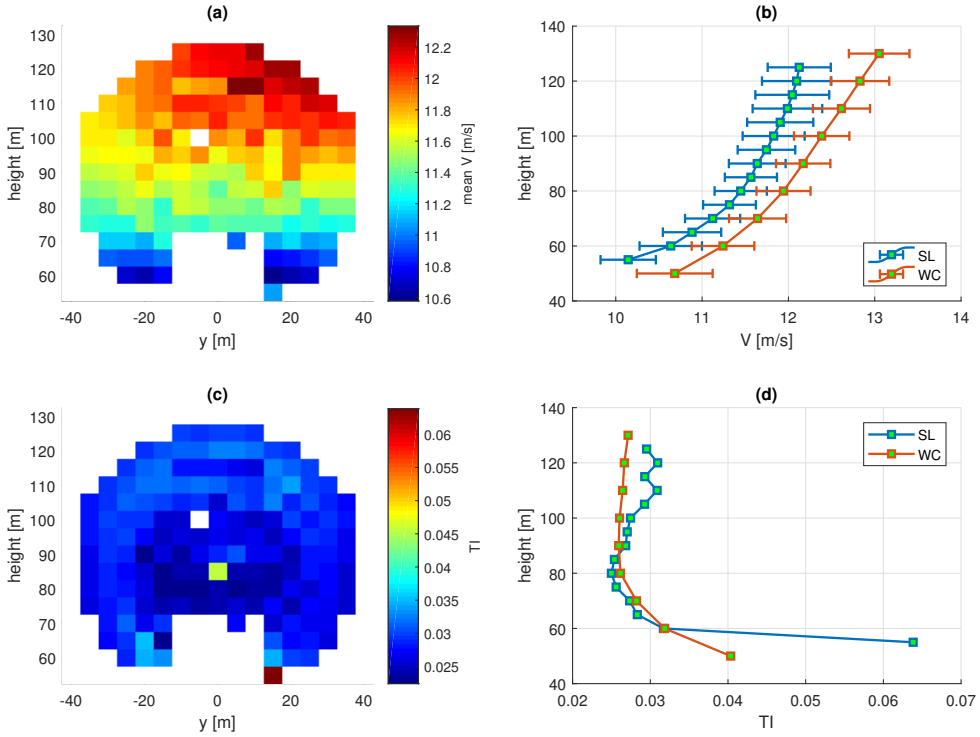

Figure E.8: Characterization of wind speed class of averaged wind speeds of 12 m/s, in total 10 periods were found for this class (see top of this Appendix for explanation on the different figures)